https://doi.org/10.5194/egusphere-2026-1312
Preprint. Discussion started: 23 March 2026
© Author(s) 2026. CC BY 4.0 License.

Incorporating Soil Organic Carbon Dynamics into Global Hydrogen Uptake Models: A Focus on Microbial Activity

Saeed Karbin[1], Julia Drewer [2], Joshua F. Dean[3], Pete Smith[1], Jo Smith[1]

[1]School of Biological Sciences, University of Aberdeen, St Machar Drive, Aberdeen, Scotland, UK

[2] UK Centre for Ecology & Hydrology, Bush Estate, Penicuik, Midlothian, Scotland, UK

[3] School of Geographical Sciences, University of Bristol, Bristol, UK

Correspondence to: Saeed Karbin (saeed.karbin@abdn.ac.uk)

Abstract

Molecular hydrogen is a secondary greenhouse gas that indirectly contributes to climate forcing by extending the atmospheric lifetime of methane through competition for hydroxyl radicals. Soil serves as a major sink for atmospheric hydrogen, making accurate estimation of soil hydrogen uptake essential for understanding its role in atmospheric chemistry. Most existing process-based models of hydrogen uptake focus primarily on abiotic controls, such as soil temperature and moisture, while either neglecting or oversimplifying the role of biotic factors, particularly microbial activity. In this study, we refine four widely used hydrogen uptake models by integrating microbial activity rate modifiers and machine learning derived soil porosity. The microbial activity rate modifiers are derived from the decomposability of soil organic carbon, which is assumed to be a proxy for potential microbial activity. This leverages simulations of soil organic matter turnover provided by well-established and tested models of soil organic matter decomposition. This simple approach enables application of hydrogen uptake models from field to global scales. We have integrated our simulations of microbial activity into four widely used hydrogen uptake models. Model performance is evaluated against empirical datasets from four detailed studies of soil hydrogen uptake. Results show that replacing traditional texture-based porosity with machine learning derived estimates significantly improved

https://doi.org/10.5194/egusphere-2026-1312
Preprint. Discussion started: 23 March 2026
© Author(s) 2026. CC BY 4.0 License.

physical transport modelling, particularly for the Bertagni and Ehhalt frameworks. Furthermore, incorporating the coupled climate-carbon microbial activity rate modifier consistently strengthened model performance, producing larger reductions in prediction error and more pronounced increases in correlation than using microbial activity alone, thereby providing a more realistic representation of soil microbial processes. These findings highlight the importance of including biologically relevant factors in atmospheric hydrogen modelling and offer a more mechanistic framework for predicting soil–atmosphere hydrogen exchange under diverse environmental conditions.

Keywords: H_2, H_2 Oxidation, H_2 model, Soil organic carbon, Maximum potential microbial activity, soil microbes

1. Introduction

Atmospheric hydrogen gas (H_2) is a naturally occurring trace gas. In 2021, the atmospheric concentration of H_2 was 552 ppb (Pétron et al. 2024). It acts as a secondary greenhouse gas (GHG) by indirectly increasing the lifetime of methane (CH_4) by competing for hydroxyl (OH) radicals that convert CH_4 to carbon dioxide. As a result, the global warming potential of H_2 is estimated to be 11.6 ± 2.8 times that of an equivalent mass of carbon dioxide (Sand et al., 2023). In addition, it contributes to the production of tropospheric ozone (O_3), water vapour and aerosols (Sand et al. 2023). Microbes in soils consume 62-92% of atmospheric H_2 losses, making soil H_2 uptake the largest and most uncertain component of the global H_2 cycle (Ouyang et al. 2025; Smith-Downey, Randerson, and Eiler 2006).

The rate and extent of H_2 oxidation in the upper soil layer are sensitive to the interplay of microbial activity, soil temperature and moisture dynamics (Constant et al. 2008; Jordaan et al. 2020; Khdhiri et al. 2015; Meredith et al. 2014). While soil moisture is essential for microbial activity, field and laboratory studies show that H_2 diffusion into the microbially active topsoil layer often limits oxidation rates. This diffusion is sensitive to soil moisture content (Buzzard et al. 2022; Smith-Downey et al. 2006). At high water levels, water-filled pore space impedes H_2 movement, slowing down H_2 uptake.

https://doi.org/10.5194/egusphere-2026-1312
Preprint. Discussion started: 23 March 2026
© Author(s) 2026. CC BY 4.0 License.

Conversely, in arid regions, insufficient moisture reduces microbial activity, eventually halting H_2 oxidation altogether. Therefore, soil moisture acts as a double-edged sword; essential for microbial life yet, in excess, a potent inhibitor of H_2 diffusion. Laboratory experiments further elucidate this interplay, revealing an optimum moisture range for H_2 uptake that varies between soil types, primarily dictated by texture and organic carbon (C) content (Conrad and Seiler 1985; 1981; Drewer et al. 2026; Ehhalt and Rohrer 2011; Reji et al. 2025; Smith-Downey et al. 2006). This intricate relationship underscores the critical role of soil moisture in regulating atmospheric H_2 uptake by soil microorganisms.

In contrast to soil water content, which influences physical and well as biological parameters, soil temperature primarily exerts its influence directly through microbial activity. Smith-Downey et al. (2006) elegantly captured this relationship using a sigmoidal function between -15 and 37°C, reflecting the gradual increase in microbial H_2 uptake with rising temperature. This finding aligns with the analysis by Ehhalt and Rohrer (2011) of diverse datasets, which revealed a consistent global pattern; negligible uptake below -20°C and above 80°C, with a broad maximum centred around 30°C. This suggests a universal optimum temperature range for microbial H_2 consumption within the soil, highlighting the importance of temperature in regulating this process.

Several studies have highlighted the influence of land use and soil organic C (SOC) content on soil H_2 uptake. Ehhalt and Rohrer (2009) observed higher H_2 dry deposition in forests compared to grasslands and agricultural lands, suggesting vegetation type plays a role in regulating this process. Land use change has also been shown to impact soil H_2 uptake, with Pendall et al. (2010) demonstrating reduced microbial oxidation rates after converting rainforest to pastures and hardwood plantations. Interestingly, Meredith et al. (2017) observed a strong covariance between soil H_2 uptake and heterotrophic soil respiration over a year at Harvard Forest in the USA, suggesting a potential link between microbial H_2 consumption and organic matter decomposition. This connection is further supported by Khdhiri et al. (2015), who identified SOC as a relatively good predictor of microbial H_2

https://doi.org/10.5194/egusphere-2026-1312
Preprint. Discussion started: 23 March 2026
© Author(s) 2026. CC BY 4.0 License.

oxidation across different land use types within the same climate. Their work also revealed that the interaction between soil C content and the relative abundance of H_2 oxidizing bacteria further improved predictions. This suggests that higher SOC may not only enhance total microbial biomass but also favour hydrogen oxidizing bacteria populations, thereby promoting H_2 consumption. While the precise mechanisms underlying the link between soil C and H_2 uptake remain unclear, it is possible that organic matter content influences H_2 oxidizing bacterial biomass through its association with overall microbial diversity (Bastida et al. 2021).

Several studies have tackled modelling soil H_2 uptake, focusing on key abiotic drivers, such as soil moisture, temperature and SOC (Bertagni et al., 2021; Dong and Layzell, 2001; Ehhalt and Rohrer, 2013; Morfopoulos et al., 2012; Paulot et al., 2021; Sanderson et al., 2003; Smith-Downey et al., 2008; Yonemura et al., 2000).

Different approaches have been used to model the impact of soil moisture on H_2 uptake. Smith-Downey *et al.* (2008) employed a simplified approach, assuming no limitation on microbial activity beyond a certain moisture level. This simplification could potentially lead to an overestimation of H_2 uptake in very wet soils. Ehhalt and Rohrer (2013) proposed a more complex two-layer model which incorporates distinct zones for H_2 transport and consumption. The first layer represents an inactive zone where H_2 diffusion occurs that can include barriers to diffusion, such as dry topsoil or snow. The second layer represents the active zone where H_2 uptake by microbes takes place. To calculate H_2 diffusion within the top 10 cm of the soil, the authors used an approach described by Millington and Quirk (1961) which considers both the air and water fractions present in the soils. Bertagni et al. (2021) introduced a novel approach to modelling soil H_2 uptake by incorporating the dependence of bacterial metabolism on soil matric potential. Their model includes two main matric potential levels; a soil water stress level that inhibits microbial activity and an optimum soil moisture condition that maximizes it. This innovative approach allows for a more nuanced representation of the interplay between soil moisture and H_2 uptake than previous models.

https://doi.org/10.5194/egusphere-2026-1312
Preprint. Discussion started: 23 March 2026
© Author(s) 2026. CC BY 4.0 License.

The diffusion of atmospheric H_2 into biologically active soil layers is a critical control on soil H_2 uptake. While existing models successfully integrate this process and some account for overlying layers, such as litter or snow (Bertagni et al., 2021; Ehhalt and Rohrer, 2013), a key challenge remains in the accurate representation of the soil pore network that transports H_2 to soil microbes. Specifically, the accurate parameterization of total soil porosity is often oversimplified. In global-scale models, porosity values are frequently assigned based solely on soil type (Morfopoulos et al. 2012; Smith Downey 2007). While this approach provides a practical way to represent soil physical properties in the model, it has significant limitations, as real-world porosity varies substantially within a soil type due to factors including SOC content, which influences microbial habitat and pore structure formation (Totsche et al. 2018; Young and Crawford 2004), land use history and management practices (Bronick and Lal 2005; Strudley et al. 2008), and compaction by agricultural machinery (Schjønning et al. 2015).

Most models use similar approaches for simulating the impact of soil temperature on H_2 uptake. Smith-Downey *et al.* (2008) introduced a sigmoidal function based on laboratory experiments to describe the temperature response between -20°C and 40°C. Ehhalt and Rohrer (2013) employed a similar function but expanded it to include a wider temperature range, exceeding 40°C.

Several models have attempted to incorporate the influence of SOC on microbial H_2 uptake. The model developed by Morfopoulos et al. (2012) considers the dynamics of soil vegetation cover, aiming to indirectly capture the effects of SOC content on H_2 uptake. In contrast, Paulot et al. (2021) adopted a modification of the Ehhalt model by introducing a constant that depends on SOC content, following a Michaelis-Menten relationship. This was a step forward in directly accounting for the impact of SOC on microbial activity but does not consider the impact of the quality of the organic matter (i.e. the decomposability of the SOC).

Here, we present a method to calculate the microbial activity rate modifier using both the quantity and quality of organic C in the soil. This is then used to refine existing calculations of H_2 uptake. The method uses simulations of SOC quality provided by the RothC model (Coleman and Jenkinson, 1996).

https://doi.org/10.5194/egusphere-2026-1312
Preprint. Discussion started: 23 March 2026
© Author(s) 2026. CC BY 4.0 License.

The RothC model estimates changes in SOC quantity and quality over time based on climate data and soil properties, including soil texture, pH, electrical conductivity (EC) and SOC content. We assume that the decomposability of SOC provides a proxy for the microbial activity and so use this to derive the microbial activity rate modifiers, which change throughout the year and at each location with changes in the quantity and quality of SOC present. This approach considers both current and historical climate and management impacts on microbial activity and calculates the relative proportions of different C pools to determine SOC quality.

By using this simple approach that can be driven by data available in individual plots as well as by data held in global databases, we retain the ability to both evaluate the model at plot scale and run simulations at large spatial scales. Therefore, these model developments can be applied to improve predictions at both field and global scale. This is crucial for assessing the indirect effect of H_2 on the climate and informing climate change mitigation strategies. Furthermore, as interest in H_2 as a clean energy carrier grows, a more comprehensive model of soil H_2 dynamics will be essential for predicting potential environmental impacts of increased emissions of H_2 to the atmosphere.

2. Methods

Note that in the following text, all symbols used are as defined in Table 1, as well as immediately below the equation.

Table 1: Nomenclature of symbols used in the H_2 oxidation models

Symbol	Definition	Units
Microbial Rate Modifier Parameters		
A	Adjustment factor (Ehhalt)	s^{-1}
$M_{C,meas}$	Measured SOC	t ha-1
$M_{C,sim}$	Simulated SOC	t ha-1
m_{CMAC}	Carbon-based microbial activity rate modifier for H_2 uptake	no units
m_{CCMAC}	Coupled climate-carbon microbial activity rate modifier for H_2 uptake	no units
M_{PI}	Estimate of plant C inputs	t ha-1
$M_{PI,start}$	Starting estimate of plant C inputs	t ha-1
N	Normalization constant such that max $(m_{MAC}) = 1$	timestep ha t-1
p_O	Fraction of organic C in soils	no units
T	Soil temperature (Morfopoulos and Ehhalt)	°C
T'	Soil temperature (Smith-Downey)	K
Model-Specific Parameters (Maximum Uptake and Rates)		
$k_{max,B}$	Maximum possible H_2 uptake (Bertagni, original)	s^{-1}
$k'_{max,B}$	Adjusted maximum H_2 uptake (Bertagni, adjusted)	s^{-1}
$k'_{max,E}$	Adjusted maximum H2 uptake (Ehhalt, adjusted)	s^{-1}

https://doi.org/10.5194/egusphere-2026-1312
Preprint. Discussion started: 23 March 2026
© Author(s) 2026. CC BY 4.0 License.

$k_{max,Mo}$	Maximum possible H_2 uptake (Morfopoulos, original)	s^{-1}
$k'_{max,Mo}$	Adjusted maximum H_2 uptake (Morfopoulos, adjusted)	s^{-1}
$k_{max,SD}$	Maximum possible H_2 uptake (Smith-Downey, original)	s^{-1}
$k'_{max,SD}$	Adjusted maximum H_2 uptake (Smith-Downey, adjusted)	s^{-1}
k_{pool}	Rate constant for decomposition of active C in pools DPM, RPM, BIO and HUM	per timestep
Response Functions (Dimensionless Modifiers)		
$m_{M,B}$	Soil moisture response modifier (Bertagni)	no units
$m_{M,E}$	Moisture rate modifier (Ehhalt)	no units
$m_{M,Ees}$	Moisture rate modifier for eolian sand (Ehhalt)	no units
$m_{M,Ell}$	Moisture rate modifier for loess loam (Ehhalt)	no units
$m_{NPP,Mo}$	Net Primary Productivity (NPP) modifier (Morfopoulos)	no units
$m_{T,E}$	Temperature rate modifier (Ehhalt)	no units
$m_{T,Mo}$	Temperature response modifier (Morfopoulos)	no units
$m_{T,SD}$	Temperature response function (Smith-Downey)	no units
Soil and Moisture Parameters		
$\beta 1$	Constant parameter (Bertagni model)	no units
$\beta 2$	Parameter dependent on $\bar{s}_{opt}$ (Bertagni model)	no units
f	Normalization constant	no units
$\bar{s}$	Relative soil water content	no units
$\bar{s}_{opt}$	Optimal soil moisture level	no units
$\bar{s}_{up}$	Upper soil moisture threshold (anoxic conditions)	no units
$\bar{s}_{ws}$	Lower soil moisture threshold (water stress)	no units
P_C	Soil organic carbon content	Percent
P_{clay}	Clay content	percent
P_{sand}	Sand content	Percent
P_{silt}	Silt content	Percent
θ_w	Volumetric moisture content	cm^3 water per cm^3 soil
θ_p	Total soil porosity	cm^3 pore space per cm^3 soil
Soil Water Retention Parameters (Bertagni Model)		
b	Empirically determined constant (grain size reflection)	no units
Ψ	Soil matric potential	Pa
$\bar{\Psi}$	Experimentally determined parameter (soil type dependent)	Pa
Ψ_{opt}	Optimal soil matric potential threshold	Pa
Ψ_{up}	Anoxic matric potential threshold	Pa
Ψ_{ws}	Water stress matric potential threshold	Pa

2.1 Estimation of Soil Porosity

Soil porosity is a critical parameter in H_2 uptake modelling, as it dictates gas diffusivity and moisture-holding capacity. In this study, we compared two distinct methods for determining soil porosity to evaluate their impact on model accuracy; a traditional texture-based approach and a contemporary machine learning-derived framework.

2.1.1 Texture-Based Porosity Estimation

In the Texture-Based (TB) approach, soil porosity was estimated based on generalized soil texture classes. Porosity values were assigned to each study site according to its dominant texture (e.g. sand, loam or clay) using physical hydrology parameters compiled by Dingman (2015). This method relies on the established physical relationship between grain size distribution and pore

https://doi.org/10.5194/egusphere-2026-1312
Preprint. Discussion started: 23 March 2026
© Author(s) 2026. CC BY 4.0 License.

space. In mineral soils, texture dictates the packing arrangement of particles; for instance, coarser soils, such as sand, typically exhibit lower total porosity compared to finer-textured soils like clay, which, despite having smaller individual pores, possess a higher total pore volume. This approach provides a deterministic baseline rooted in classical soil physics.

2.1.2 Machine Learning Approach

To capture the complex, non-linear relationships between soil structure and environmental variables, a machine learning (ML) approach was employed to estimate soil porosity. In this method, the saturated soil water content was used as a direct proxy for total soil porosity. The ML approach integrates these complex relationships through tree-based ensemble models, such as Random Forest and Gradient Boosting, as detailed in the SoilGrids framework (Hengl et al. 2017). By leveraging a massive global soil profile database, incorporating variables, such as texture, organic matter, topography, and climate, this method produces spatially detailed and realistic porosity estimates. Unlike the TB method, the ML approach accounts for localized environmental heterogeneity, potentially offering a more robust input for H_2 uptake simulations.

2.2 Simulation of Microbial Activity Rate Modifier for Hydrogen Uptake

The microbial activity rate modifier of the soil was simulated on a monthly timestep following the approach used in the well-established RothC model (Coleman and Jenkinson, 1996). The microbial activity rate modifier is described by simulating the proportion of the SOC that resides in organic matter pools of different decomposability; decomposable plant material (DPM), resistant plant material (RPM), microbial biomass (BIO), humified organic matter (HUM) and inert organic matter (IOM). These pools have different decomposition rate constants, and so the proportion of SOC in each pool determines the overall decomposability of the organic matter in the soil. Because the organic matter feeds the microorganisms, after accounting for factors affecting bioavailability (such as physical protection), organic matter decomposability can be taken as a surrogate for the potential microbial activity.

https://doi.org/10.5194/egusphere-2026-1312
Preprint. Discussion started: 23 March 2026
© Author(s) 2026. CC BY 4.0 License.

As is normal practice with RothC simulations (e.g. Abegaz et al., 2016), the organic matter decomposability at the start of the simulation was determined from the measured values of SOC using a spin-up of the SOC pools to steady state (where a soil in steady state is no longer undergoing long-term change in SOC due to previous land use change). In this approach, the simulations are run from a starting point of a soil containing no C, using default values of plant inputs within the model. The simulations are continued, using repeated weather data, until the simulated SOC stops changing. The simulated and measured steady state values of SOC are then compared and the default plant inputs adjusted as shown below:

$$M_{\mathrm{PI}} = M_{\mathrm{PI,start}} \times {M_{\mathrm{C,meas}}}/{M_{\mathrm{C,sim}}} \quad (1)$$

where M_{PI} is the revised estimate of plant C inputs, $M_{\mathrm{PI,start}}$ is the starting estimate of plant C inputs, $M_{\mathrm{C,meas}}$ is the measured SOC, and $M_{\mathrm{C,sim}}$ is the simulated SOC (all in t ha^{-1}). This process is continued until the value of M_{PI} no longer changes and $M_{\mathrm{C,meas}}$ = $M_{\mathrm{C,sim}}$. At this point, the simulation is considered to be at steady state, and so the combined decomposability of the simulated SOC pools can be assumed to provide a good estimate of the overall bioavailability of the SOC. Because the spin-up process determines the proportions of the different pools, it implicitly accounts for factors affecting bioavailability. Running the model forwards using changes in weather and management conditions is then used to estimate changes in SOC over time. This has been shown in many earlier studies to provide an accurate simulation of changes in SOC (Abdalla et al. 2014; Dondini et al. 2017; Dondini et al. 2016a; Dondini et al. 2016b; Dondini et al. 2015; Gottschalk et al. 2012; Smith et al. 2020).

This carbon-based microbial activity was then converted into a rate modifier for H_2 uptake, m_{CMAC}, (no units) accounting for the impacts on H_2 uptake of SOC quantity and quality in each month during the forward run as shown below:

$$m_{\mathrm{CMAC}} = \frac{1}{N} \sum_{\mathrm{pool}} C_{\mathrm{pool}} \left(1 - \exp\left(-k_{\mathrm{pool}}\right)\right) \quad (2)$$

https://doi.org/10.5194/egusphere-2026-1312
Preprint. Discussion started: 23 March 2026
© Author(s) 2026. CC BY 4.0 License.

where N is a normalization constant (timestep ha t^{-1}), such that max (m_{CMAC}) = 1 (no units), C_{pool} is the mass of total active C in the pools DPM, RPM, BIO and HUM (t ha^{-1}) and k_{pool} is the rate constant for decomposition of active C in pools DPM, RPM, BIO and HUM (per timestep). The values of the rate constants, k_{DPM}, k_{RPM}, k_{BIO} and k_{HUM}, were obtained from Coleman & Jenkinson, (1996) and are set to 10, 0.3, 0.66 and 0.02 y^{-1}, respectively. The rate constants were converted to the timestep being used in the particular simulation by multiplying by the number of days in the timestep and dividing by 365 days per year. The timestep selected depends on the frequency of measurements available for model evaluation (in this study it is monthly).

2.2.1 Incorporating Hydrogen Oxidation Activity in Established Models

The microbial activity rate modifier for H_2 uptake (m_{CMAC}) was incorporated into the established models provided by Smith-Downey (2007), Morfopoulos et al. (2012), Ehhalt and Rohrer (2013) and Bertagni et al. (2021) to evaluate the impact of including microbial activity on the outputs from each model. The following sections provide detailed descriptions of the approaches used to translate m_{CMAC} into the H_2 oxidation activity for each model.

Smith-Downey Model

Smith-Downey (2007) estimated H_2 oxidation activity, k (s^{-1}), using a model relying solely on the abiotic factors, soil moisture, temperature and SOC (Eq. 3).

$$k = k_{\mathrm{max,SD}} \times m_{\mathrm{T,SD}} \times m_{\mathrm{M,SD}} \times m_{\mathrm{O,SD}} \quad (3)$$

where $k_{\mathrm{max,SD}}$ is the maximum possible H_2 uptake (s^{-1}) under ideal soil temperature and moisture conditions (derived from lab measurement to be 0.012266 s^{-1}), $m_{\mathrm{T,SD}}$ and $m_{\mathrm{M,SD}}$ (no units) are response functions to soil temperature and moisture, respectively, ranging between 0 and 1, and $m_{\mathrm{O,SD}}$ (no units) is the response function to SOC.

The response to temperature $m_{\mathrm{T,SD}}$ is a sigmoidal function with the following parameters:

https://doi.org/10.5194/egusphere-2026-1312
Preprint. Discussion started: 23 March 2026
© Author(s) 2026. CC BY 4.0 License.

$$m_{\mathrm{T,SD}} = {}^{1}/_{(1+\exp(-0.1718\times T'+46.938))} \quad (4)$$

where T' is the soil temperature (K).

The response to moisture $m_{\mathrm{M,SD}}$ is given by $m_{\mathrm{M,SD}} = 0$ when soil moisture is below 8% saturation, $m_{M,\mathrm{SD}} = 14.286 \times \bar{s} - 1.1429$ between 8% and 15% saturation and $m_{\mathrm{M}} = 1$ above 15% saturation, where $\bar{s}$ is relative water content (no units).

The response function to SOC is calculated by the following equation:

$$m_{\mathrm{O,SD}} = 1.178 \times p_{\mathrm{O}} + 0.3465 \quad (5)$$

where p_{O} is a fraction of organic C in the soil.

The original H_2 oxidation activity (Eq. 3) was adapted to include microbial activity (m_{CMAC}) as shown in Eq. 6:

$$k = k'_{\mathrm{max,SD}} \times m_{\mathrm{T,SD}} \times m_{\mathrm{M,SD}} \times m_{\mathrm{CMAC}} \quad (6)$$

where $k'_{\mathrm{max,SD}}$ (s^{-1}) is maximum potential H_2 uptake needed to ensure that the global average H_2 oxidation activity (k) remains equivalent across the original and the new formulations (thereby preserving the established atmospheric H_2 budget). The value of $k'_{\mathrm{max,SD}}$ was calculated using the global average of the existing parameters ("ave" in equation 7 denotes the global average):

$$k'_{\mathrm{max,SD}} = \frac{\mathrm{ave}(k_{\mathrm{max,SD}}\times m_{\mathrm{T,SD}}\times m_{\mathrm{M,SD}}\times m_{\mathrm{O,SD}})}{\mathrm{ave}(m_{\mathrm{T,SD}}\times m_{\mathrm{M,SD}}\times m_{\mathrm{CMAC}})} = \frac{\mathrm{ave}(k_{\mathrm{max,SD}}\times m_{\mathrm{O,SD}})}{\mathrm{ave}(m_{\mathrm{CMAC}})} \quad (7)$$

This approach provided a value for the adjusted maximum potential H_2 uptake of $k'_{\mathrm{max,SD}} = 0.0058\ s^{-1}$. The value of $k'_{\mathrm{max,SD}}$ is 47% of the original value of $k_{\mathrm{max,SD}}$, reflecting the greater sensitivity of the revised model to microbial activity than the original model to SOC. Monthly soil temperature and soil moisture were derived from the ERA5 reanalysis product (Hersbach et al. 2023). Data on SOC were obtained from the FAO global soil database (FAO 2017).

https://doi.org/10.5194/egusphere-2026-1312
Preprint. Discussion started: 23 March 2026
© Author(s) 2026. CC BY 4.0 License.

Morfopoulos Model

Morfopoulos et al. (2012) calculated H_2 oxidation activity (k) as:

$$k = k_{\mathrm{max,Mo}} \times m_{\mathrm{T,Mo}} \times m_{\mathrm{M,SD}} \times m_{\mathrm{NPP,Mo}} \quad (8)$$

where $k_{\mathrm{max,Mo}}$ is the maximum possible H_2 uptake (s^{-1}), which was derived by adjusting the global mean uptake estimated for the 1991–2006 period to align with the value reported by Bousquet et al. (2011). This adjustment gave a $k_{\mathrm{max,Mo}}$ value of 0.038 s^{-1}.

The temperature response modifier, $m_{\mathrm{T,Mo}}$ (no units) accounts for the influence of soil temperature on H_2 uptake and is defined over the range of –15 °C to 40 °C using the empirical function proposed by Smith Downey, (2007). Outside the range of –15 °C to 80 °C, $m_{\mathrm{T,Mo}}$ is set to zero. Within the broader range of 40 °C to 80 °C, $m_{\mathrm{T,Mo}}$ is calculated as:

$$m_{\mathrm{T,Mo}} = -0.25(T' + 273.15) + 8.83 \quad (9)$$

where T' is the soil temperature (°C).

The soil moisture response modifier ($m_{\mathrm{M,SD}}$) is calculated as given by Smith-Downey model. The net primary production (NPP) modifier ($m_{\mathrm{NPP,Mo}}$) serves as a proxy for SOC availability. In this model, regions where the annual NPP is less than 10 g C m^{-2} y^{-1} are masked by setting $m_{\mathrm{NPP,Mo}} = 0$, excluding arid or desert environments from the modelled uptake. Conversely, for areas with NPP values equal to or exceeding this threshold, $m_{\mathrm{NPP,Mo}} = 1$.

To include the microbial activity rate modifier (m_{CMAC}) into this model, we used a similar approach to that used for the Smith-Downy model to calculate a new, adjusted value for the maximum potential H_2 uptake, $k'_{\mathrm{max,Mo}}$ (s^{-1}). The original H_2 oxidation activity (Eq.8) was modified to include the microbial activity rate modifier as:

$$k = k'_{\mathrm{max,Mo}} \times m_{\mathrm{T,Mo}} \times m_{\mathrm{M,SD}} \times m_{\mathrm{CMAC}} \quad (10)$$

To ensure that the global average H_2 oxidation activity (k) remained equivalent across the original and the new formulations, $k'_{\mathrm{max,Mo}}$ was recalculated using the global average of the existing parameters:

https://doi.org/10.5194/egusphere-2026-1312
Preprint. Discussion started: 23 March 2026
© Author(s) 2026. CC BY 4.0 License.

$$k'_{\mathrm{max,Mo}} = \frac{\mathrm{ave}(k_{\mathrm{max,Mo}} \times m_{\mathrm{T,Mo}} \times m_{\mathrm{M,SD}} \times m_{\mathrm{NPP,Mo}})}{\mathrm{ave}(m_{\mathrm{T,Mo}} \times m_{\mathrm{M,SD}} \times m_{\mathrm{CMAC}})} = \frac{\mathrm{ave}(k_{\mathrm{max,Mo}} \times m_{\mathrm{NPP,Mo}})}{\mathrm{ave}(m_{\mathrm{CMAC}})} \quad (11)$$

This gave a new value for $k'_{\mathrm{max,Mo}}$ of 0.0437 s^{-1}. This is only 15% higher than the value of $k_{\mathrm{max,Mo}}$ in the original model, reflecting similar sensitivities to microbial activity and NPP in the two versions.

Monthly NPP data were obtained from the LPJ dynamic global vegetation model as part of the TRENDYv10 project (Poulter 2021). Soil temperature and soil moisture data were extracted from LPJ-GUESS model outputs (scenario S0) developed by the Karlsruhe Institute of Technology (KIT), Germany (Anthoni 2021). For all datasets, data from the year 2007 were employed, consistent with Morfopoulos et al. (2012), who calculated $k_{\mathrm{max,Mo}}$ by adjusting the global mean uptake as reported by Bousquet et al. (2011).

Ehhalt Model

Ehhalt and Rohrer (2013) calculated k (s^{-1}) as:

$$k = A \times m_{\mathrm{T,E}} \times m_{\mathrm{M,E}} \quad (12)$$

where A (s^{-1}) is an adjustment factor designed to scale the model to specific soil biological, chemical and physical conditions based on empirical measurements (here we assumed $A = 1$ to provide a standardized baseline for evaluating the functional sensitivity of the modifiers without the influence of site-specific calibration factors), $m_{\mathrm{T,E}}$ is the temperature rate modifier and $m_{\mathrm{M,E}}$ is the moisture rate modifier (no units). The value of $m_{\mathrm{T,E}}$ is calculated as:

$$m_{\mathrm{T,E}} = \left(1 \Big/ \left(1 + \exp\left(\frac{-(T'-3.8)}{6.7} \right) \right) \right) + \left(1 \Big/ \left(1 + \exp\left(\frac{(T'-62.2)}{7.1} \right) \right) \right) - 1 \quad (13)$$

where T' is temperature (°C).

The value of $m_{\mathrm{M,E}}$ differs between soil types, and can be calculated for eolian sand ($m_{\mathrm{M,E\,es}}$) and for loess loam ($m_{\mathrm{M,E\,ll}}$) as:

https://doi.org/10.5194/egusphere-2026-1312
Preprint. Discussion started: 23 March 2026
© Author(s) 2026. CC BY 4.0 License.

$$m_{\mathrm{M,E\ es}} = \left.0.00936 \times \left(\frac{\theta_{\mathrm{w}}}{\theta_{\mathrm{p}}} - 0.0264\right) \times \left(1 - \frac{\theta_{\mathrm{w}}}{\theta_{\mathrm{p}}}\right)\right/ \left(\frac{\theta_{\mathrm{w}}}{\theta_{\mathrm{p}}}\right)^2 - 0.1715 \times \left(\frac{\theta_{\mathrm{w}}}{\theta_{\mathrm{p}}}\right) + 0.03144 \quad (14)$$

$$m_{\mathrm{M,E\ ll}} = \left.0.01997 \times \left(\frac{\theta_{\mathrm{w}}}{\theta_{\mathrm{p}}} - 0.05369\right) \times \left(0.8508 - \frac{\theta_{\mathrm{w}}}{\theta_{\mathrm{p}}}\right)\right/ \left(\frac{\theta_{\mathrm{w}}}{\theta_{\mathrm{p}}}\right)^2 - 0.7541 \times \left(\frac{\theta_{\mathrm{w}}}{\theta_{\mathrm{p}}}\right) + 0.2806 \quad (15)$$

where Θ_{w} is the volumetric moisture content (cm³ of water filled pores per cm³ soil) and Θ_{p} is total soil porosity of the soil (cm³ total pore space per cm³ soil).

To add the microbial activity rate modifier (m_{CMAC}) to this model, we calculated a new adjustment factor, $k'_{\mathrm{max,E}}$. The original H_2 oxidation activity (Eq. 12) was modified to include the microbial activity rate modifier as shown in Eq. 16:

$$k = k'_{\mathrm{max,E}} \times m_{\mathrm{T,E}} \times m_{\mathrm{M,E}} \times m_{\mathrm{CMAC}} \quad (16)$$

To ensure that the global average H_2 oxidation activity (k) remained equivalent across the original and the new formulations, $k'_{\mathrm{max,E}}$ was calculated using the global average of the existing parameters:

$$k'_{\mathrm{max,E}} = \frac{\mathrm{ave}(m_{\mathrm{T,E}} \times m_{\mathrm{M,E}})}{\mathrm{ave}(m_{\mathrm{T,E}} \times m_{\mathrm{M,E}} \times m_{\mathrm{CMAC}})} = \frac{1}{\mathrm{ave}(m_{\mathrm{CMAC}})} \quad (17)$$

This gave a value of $k'_{\mathrm{max,E}}$ 1.2569 s^{-1}, which is 26% higher than the original value of A, reflecting the added response in the new model to microbial activity that was neglected in the original. Soil temperature and soil moisture data were extracted from the ERA5 reanalysis product (Hersbach et al. 2023).

Bertagni model

Following the common approach of Smith-Downey and Ehhalt models, Bertagni et al. (2021) assumed soil microbial H_2 oxidation activity is expressed as shown below:

$$k = k_{\mathrm{max,B}} \times m_{\mathrm{T,E}} \times m_{\mathrm{M,B}} \quad (18)$$

https://doi.org/10.5194/egusphere-2026-1312
Preprint. Discussion started: 23 March 2026
© Author(s) 2026. CC BY 4.0 License.

where $k_{\max,B}$ is the maximum possible H_2 uptake (s^{-1}) under optimum conditions which is assigned a value of 0.03 s^{-1}, $m_{T,E}$ (no units) is calculated by the formula suggested by Ehhalt and Rohrer, (2011) in Eq. 13, and $m_{M,B}$ (no units) is calculated as expressed below:

$$m_M = \frac{1}{f}\,(\bar{s} - \bar{s}_{ws})^{\beta 1}(\bar{s}_{up} - \bar{s})^{\beta 2} \quad (19)$$

where $\bar{s}$ is relative soil water content ($\bar{s} = 0$ for dry soil and $\bar{s} = 1$ for saturated soil, no units). $\bar{s}_{ws}$ and $\bar{s}_{up}$ are the soil-dependent lower and upper soil moisture thresholds for microbial activity, respectively (no units) and f is a normalization constant (no units) such that $\max(m_M) = 1$. The beta parameters are set to impose a maximum value for $\beta 2$ (no units) at $\bar{s} = \bar{s}_{opt}$, that is,

$$\beta 2 = \beta 1(1 - \bar{s}_{opt})/(\bar{s}_{opt} - \bar{s}_{ws}) \quad (20)$$

where β1 is a constant value of 0.4 (no units), $\bar{s}_{opt}$ is soil matric potential at which microbial activity is most favoured (no units) and $\bar{s}_{ws}$ is the soil matric potential where activity is inhibited by water stress (no units).

In this model, the authors explore the impact of soil texture on microbial activity through the lens of the soil matric potential. The authors identified specific matric potential thresholds associated with optimal bacterial activity, Ψ_{opt} (Pa), water stress-induced limitations, Ψ_{ws} (Pa) and anoxic conditions, Ψ_{up} (Pa), offering valuable insights into how soil moisture availability influences microbial communities. The connection between matric potential and relative soil moisture is established through the soil water retention curve, as described by Campbell (1974):

$$\Psi = \tilde{\Psi} \times \bar{s}^{-b} \quad (21)$$

where $\tilde{\Psi}$ is an experimentally determined parameter that depends on soil type (Pa). The absence of activity is assumed to occur at the wilting point, corresponding to approximately -3 MPa, giving the $\bar{s}_{ws}$ values for various soil types. For the upper limit, previous studies (Conrad & Seiler, 1981; Smith-Downey et al., 2006) indicate no inhibition up to saturation, leading to a fixed $\bar{s}_{up} = 1$. The optimal

https://doi.org/10.5194/egusphere-2026-1312
Preprint. Discussion started: 23 March 2026
© Author(s) 2026. CC BY 4.0 License.

condition for activity (Ψ_{opt}), estimated by averaging experimental data from diverse sources, falls around -0.3 MPa (Conrad and Seiler, 1981; Smith-Downey et al., 2006). Finally, the value of b , which reflects the grain size of the different soil types, is an empirically determined constant (Campbell, 1974).

To incorporate the microbial activity rate modifier for H_2 uptake (m_{CMAC}) into this model, we calculated a new, adjusted value for the maximum potential H_2 uptake ($k'_{max,B}$). The original H_2 oxidation activity (Eq.18) was modified to include microbial activity (m_{CMAC}) as:

$$k = k'_{max,B} \times m_{T,E} \times m_{M,B} \times m_{CMAC} \quad (22)$$

To ensure that the global average H_2 oxidation activity (k) remained equivalent across the original and the new formulations, $k'_{max,B}$ was calculated using the global average of the existing parameters ("ave" means global average):

$$k'_{max,B} = \frac{ave(k_{max,B} \times m_{T,E} \times m_{M,B})}{ave(m_{T,E} \times m_{M,B} \times m_{CMAC})} = \frac{ave(k_{max,B})}{ave(m_{CMAC})} \quad (23)$$

This gave a value for the adjusted maximum potential H_2 uptake ($k'_{max,B}$) of 0.0437 s^{-1}. This 46% increase in the value of $k'_{max,B}$ compared to $k_{max,B}$ reflects the added response of the model to microbial activity. Soil temperature and soil moisture data were extracted from the ERA5 reanalysis product (Hersbach et al. 2023).

2.2.2 Improved Description of Environmental Impacts on Microbial Activity

Building on the carbon-based microbial activity rate modifier (m_{CMAC}) described in Section 2.1, improved descriptions of environmental controls, temperature ($m_{T,E}$) and soil moisture ($m_{M,B}$), were incorporated into the calculation as:

$$m_{CCMAC} = \frac{1}{N} \sum_{pool} C_{pool} \left(1 - \exp\left(-m_{T,E} \times m_{M,B} \times k_{pool}\right)\right) \quad (24)$$

where m_{CCMAC} is the coupled climate-carbon microbial activity rate modifier for H_2 uptake, in which environmental controls ($m_{T,E}$ and $m_{M,B}$) are included within the calculation of the rate modifier. All

https://doi.org/10.5194/egusphere-2026-1312
Preprint. Discussion started: 23 March 2026
© Author(s) 2026. CC BY 4.0 License.

terms and constants follow the definitions provided in Section 2.1. The soil water thresholds ($\bar{s}_{ws}$ and $\bar{s}_{opt}$) for $m_{M,B}$ are calculated using pedotransfer functions (PTFs) presented by Brand et al. (2020). These thresholds are relative water content (no units) and determined as follows:

$$\bar{s}_{ws} = r4\left(9.878 + 0.2127P_{clay} - 0.08366P_{silt} - 7.67\left(1/(1+P_C)\right) + 0.003853P_{silt}P_{clay} + 0.233\,P_{clay}\left(1/(1+P_C)\right) + 0.09498\,P_{silt}\left(1/(1+P_C)\right)\right)/100 \quad (25)$$

$$\bar{s}_{opt} = \left(24.49 - 18.87\left(1/(1+P_C)\right) + 0.4527P_{clay} + 0.1535P_{silt} + 0.1442\,P_{silt}\left(1/(1+P_C)\right) - 0.00511P_{silt}P_{clay} + 0.08676P_{clay}\left(1/(1+P_C)\right)\right)/100 \quad (26)$$

where P_{clay}, P_{silt} and P_C represent soil clay, silt and organic C content, respectively. The unit for all values is percentage by weight (%). Including these $m_{T,E}$ and $m_{M,B}$ within the exponential term for each pool increases the impact of the soil quality on the moisture and temperature responses, as demonstrated in Fig. 7.

As in Section 2.1.1, m_{CCMAC} was incorporated into the four established models (Smith-Downey, Morfopoulos, Ehhalt, Bertagni) by replacing original formulations with:

$$k = k'_{max} \times m_{CCMAC} \quad (28)$$

where k'_{max} represents $k'_{max,SD}$, $k'_{max,Mo}$, $k'_{max,E}$ and $k'_{max,B}$, respectively. Note that the temperature and moisture rate modifiers in the original models are now not included as they are already accounted for inside the exponential term.

The recalculated k'_{max} values ensured global H_2 uptake remained consistent with original budgets, using the same averaging approach described in Section 2.1.1. This calculation produced values of k'_{max}= 0.007, 0.059, 0.02, and 0.035 s^{-1} for the Smith-Downey, Morfopoulos, Ehhalt and Bertagni models, respectively. This reflects an increased impact of m_{CCMAC} in the Smith-Downey and Morfopoulos models compared to the impact of m_{CMAC}, but a reduced impact in the Ehhalt and Bertagni models.

https://doi.org/10.5194/egusphere-2026-1312
Preprint. Discussion started: 23 March 2026
© Author(s) 2026. CC BY 4.0 License.

Environmental data sources (ERA5 for temperature/moisture, FAO for SOC, LPJ for NPP) and calibration procedures were consistent with those outlined in Section 2.1.

2.3. Evaluation of Model Performance

2.3.1 Data Sources

The data used for model evaluation were obtained from a detailed review of the literature. Soil H_2 flux measurements from a garden meadow (Bartyzel et al., 2013) and an urban forest (Lallo et al., 2008) were obtained directly from the respective publications. Soil moisture and temperature data corresponding to these study locations and measurement periods were extracted from Hersbach et al. (2023) and are provided in Table 2. In addition, flux measurements from grassland and forest sites reported by Cowan et al. (2025) were used to evaluate model performance.

Soil properties including soil texture, bulk density and SOC were derived from two distinct sources. For three datasets, Harvard Forest (L. Meredith, Wofsy, and Prinn 2023), Lallo et al. (2008) and Bartyzel et al. (2013), soil properties were extracted from the Harmonized World Soil Database (HWSD; Nachtergaele et al., 2010). Data for the grassland and forest sites described by Cowan et al. (2025) were sourced directly from published measurements, as detailed in Table 2.

https://doi.org/10.5194/egusphere-2026-1312
Preprint. Discussion started: 23 March 2026
© Author(s) 2026. CC BY 4.0 License.

Table 2: Summary of measurement details for the datasets used in models' evaluation across various studies. Note: SOC denotes soil organic C.

Study site	Location	Land use	Soil type	SOC (%)	Method	Measurement period
Bartyzel et al. (2013)	Krakow, Poland	Garden meadow	Loam	2.59	Static chamber	Nov. 2011 -Jun. 2012
Cowan et al. (2025) a	Edinburgh, UK	Grassland	Clay	4	Static chamber	Sep. 2023- Sep. 2024
Cowan et al. (2025) b	Edinburgh, UK	Forest	Sandy clay loam	3.1	Static chamber	Sep. 2023- Sep. 2024
Lallo et al. (2008)	Helsinki, Finland	Forest	Loamy sand	2.46	Static chamber	Aug. 2005 -Mar. 2007
Meredith et al. (2017)	Massachusetts, USA	Forest	Loamy Sand	5.57	Gradient flux measurement	Feb. 2011 – Jan. 2012

Table 3: Key soil properties of the datasets utilized for evaluating the models' performance.

Study site	Soil pH	Clay (%)	Sand (%)	Silt (%)	Bulk density (g cm^{-3})	Texture-derived (cm^3 cm^{-3})		PTFs-derived (cm^3 cm^{-3})		Total porosity (cm^3 cm^{-3})	
						$\bar{S}_{ws}$	$\bar{S}_{opt}$	$\bar{S}_{ws}$	$\bar{S}_{opt}$	Texture-derived	ML -derived
Bartyzel et al. (2013)	6.2	22	41	37	1.34	0.24	0.37	0.16	0.32	0.41	0.46
Cowan et al. (2025, Grassland)	5.5	55	25	20	1.11	0.53	0.64	0.25	0.44	0.5	0.56
Cowan et al. (2025, Forest)	5.3	25	60	15	0.96	0.32	0.44	0.15	0.32	0.4	0.56
Lallo et al. (2008)	4.8	25.7	37.6	36.7	0.85	0.11	0.18	0.09	0.26	0.42	0.62
Meredith et al. (2017)	5.3	5	85	10	1.7	0.11	0.18	0.09	0.25	0.43	0.55

*Table 4: Summary of model formulations before and after the inclusion of the coupled climate-carbon microbial activity rate modifier (m_{CCMAC}) in different models. *, in this study $A = 1\ s^{-1}$.*

Model	Original models	k'_{max}	m_{CCMAC}
Smith-Downey	$k = k_{\max,SD} \times m_{T,SD} \times m_{M,SD} \times m_{O,SD}$	0.007	$k = k'_{\max,SD} \times m_{CCMAC}$
Morfopoulos	$k = k_{\max,Mo} \times m_{T,Mo} \times m_{M,SD} \times m_{NPP,Mo}$	0.059	$k = k'_{\max,MO} \times m_{CCMAC}$
Ehhalt	$k = A^* \times m_{T,E} \times m_{M,E}$	0.020	$k = k'_{\max,E} \times m_{CCMAC}$
Bertagni	$k = k_{\max,Mo} \times m_{T,E} \times m_{M,B}$	0.035	$k = k'_{\max,B} \times m_{CCMAC}$

In addition, we sourced data from the continuous, year-long measurements (December 2010 – February 2012) collected at the Harvard Forest in Petersham, Massachusetts, USA. These measurements provided the average daily deposition velocity (L. Meredith, Wofsy, and Prinn 2023). The Harvard Forest is a predominantly deciduous forest with trees aged 80-115 years old. Dominant tree species include red oak, red maple, red and white pine, and hemlock (Meredith et al., 2014). Notably, this dataset represents one of the most extensive field-based measurements of soil-atmosphere H_2 flux to date. Soil temperature and moisture data for this study were obtained from the Harvard Forest Long-Term Ecological Research (LTER) datasets HF018 (Fery and Melillo, 2025).

The saturated soil water content was derived using a machine learning approach (Hengl et al. 2017), providing a proxy for total soil porosity.

https://doi.org/10.5194/egusphere-2026-1312
Preprint. Discussion started: 23 March 2026
© Author(s) 2026. CC BY 4.0 License.

2.3.2 Data Extraction

We used free online plotting and digitization software, WebPlotDigitizer (Rohatgi, 2022), to extract data on soil H_2 uptake and associated soil parameters from Lallo et al. (2008) and Bartyzel et al. (2013) measurements. The software allows users to upload an image of a graph, calibrate the axes, plot the data points, and export the (x,y) coordinate data to Microsoft Excel. To facilitate a month-by-month comparison of the outputs from different models, we computed monthly averages for H_2 deposition velocity, soil temperature and soil moisture (Table 5-10). The model performance was assessed using the approach laid out by Smith and Smith (2007).

Table 5: Soil temperature, soil moisture and deposition velocity of H2 measured by Bartyzel et al. (2013) using the static chamber method in a garden meadow (partly covered by trees) in Krakow, Poland. Average monthly data is calculated.

Date	Temperature (°C)	Moisture (v/v)	Deposition Velocity (cm s^{-1})
Nov-2011	2.20	0.21	0.03
Dec-2011	2.10	0.34	0.02
Jan-2012	2.10	0.44	0.02
Feb-2012	-4.90	0.36	0.01
Mar-2012	4.72	0.39	0.02
Apr-2012	10.65	0.35	0.03
May-2012	15.57	0.27	0.04
Jun-2012	20.04	0.27	0.05

Table 6: Deposition velocity of H_2 measured by Meridith et al (2023) in Harvard Forest using the gradient method. Average monthly data is calculated.

Date	Temperature (°C)	Moisture (v/v)	Deposition Velocity (cm s^{-1})
Dec-2010	2.06	0.29	0.0131
Jan-2011	0.31	0.28	0.0064
Feb-2011	1.07	0.29	0.0035
Mar-2011	1.36	0.37	0.0052
Apr-2011	4.28	0.37	0.0103
May-2011	10.6	0.32	0.0108
Jun-2011	16.2	0.27	0.0253
Jul-2011	18.2	0.24	0.0398
Aug-2011	19.1	0.22	0.0382
Sep-2011	16.9	0.26	0.0311
Oct-2011	15.2	0.28	0.0234
Nov-2011	7.71	0.28	0.0165
Dec-2011	5.5	0.30	0.0115
Jan-2012	2.14	0.30	0.0079

https://doi.org/10.5194/egusphere-2026-1312
Preprint. Discussion started: 23 March 2026
© Author(s) 2026. CC BY 4.0 License.

Table 7: Digitized soil temperature, soil moisture and deposition velocity of H_2 measured by Bartyzel et al. (2013) using the static chamber method in a garden meadow in Krakow, Poland. Average monthly data is calculated.

Date	Temperature (°C)	Moisture (v/v)	Deposition Velocity (cm s^{-1})
Nov-2011	2.20	0.21	0.03
Dec-201	2.10	0.35	0.02
Jan-2012	2.10	0.44	0.02
Feb-2012	-4.90	0.37	0.01
Mar-2012	4.72	0.40	0.02
Apr-2012	10.65	0.35	0.03
May-2012	15.57	0.28	0.04
Jun-2012	20.04	0.27	0.05

Table 8: Deposition velocity of H_2 measured by Cowan et al (2025) in a grassland using the static chambers. Average monthly data is calculated.

Date	Temperature (°C)	Moisture (v/v)	Deposition Velocity (cm s^{-1})
Sep-2023	13.22	0.33	0.0214
Oct-2023	9.77	0.40	0.0092
Nov-2023	6.62	0.45	0.0020
Jan-2024	3.31	0.44	0.0015
Feb-2024	2.93	0.45	0.0042
Mar-2024	8.58	0.44	0.0035
Apr-2024	8.24	0.42	0.0052
May-2024	14.01	0.31	0.0247
Jun-2024	16.66	0.26	0.0326
Jul-2024	15.49	0.31	0.0286
Aug-2024	15.02	0.34	0.0019
Sep-2024	10.26	0.33	0.0031

Table 9: Deposition velocity of H_2 measured by Cowan et al (2025) in a forest using the static chambers. Average monthly data is calculated.

Date	Temperature (°C)	Moisture (v/v)	Deposition Velocity (cm s^{-1})
Sep-2023	13.96	0.13	0.1085
Nov-2023	6.72	0.33	0.0751
Feb-2024	5.60	0.33	0.0804
Apr-2024	6.46	0.36	0.0848
May-2024	12.38	0.27	0.1172
Jun-2024	10.17	0.26	0.0924
Jul-2024	11.69	0.11	0.0781
Aug-2024	13.50	0.15	0.1206
Sep-2024	11.21	0.24	0.0818

Table 10: Digitized soil temperature, soil moisture and deposition velocity of H_2 measured by Lallo et al. (2008) using the static chamber method in an urban forest in Helsinki, Finland. Average monthly data is calculated.

Date	Temperature (°C)	Moisture (v/v)	Deposition Velocity (cm s^{-1})
Aug-2005	17.98	0.2	0.0524
Sep-2005	13.65	0.28	0.0531
Oct-2005	8.51	0.35	0.0346
Dec-2005	3.01	0.37	0.0197
Jan-2006	-0.76	0.37	0.0014
Feb-2006	-7.55	0.35	0.0001
Mar-2006	1.18	0.36	0.0000
Apr-2006	3.91	0.3	0.0435
May-2006	8.77	0.31	0.0561
Jun-2006	14.08	0.25	0.0701
Aug-2006	17.27	0.29	0.0510
Nov-2006	1.75	0.35	0.0312
Dec-2006	1.64	0.36	0.0392

https://doi.org/10.5194/egusphere-2026-1312
Preprint. Discussion started: 23 March 2026
© Author(s) 2026. CC BY 4.0 License.

2.3.3 Evaluation

The model evaluation used the procedures set out by Smith et al. (1996). The level of agreement between the simulated and measured deposition velocities was first assessed graphically by plotting simulations and measurements against time. The level of agreement between the simulated and measured deposition velocities was assessed statistically using the root-mean-square error, E_{RMSE} (%), expressed as

$$E_{\mathrm{RMSE}} = \sqrt{\frac{\overline{|S_i - O_i|}}{\overline{O_i}}} \times 100 \quad (21)$$

where S_i is the simulated value for soil H_2 uptake (cm s^{-1}), O_i is the observed (measured) H_2 uptake in the soil (cm s^{-1}). A lower value of E_{RMSE} indicates better model performance.

The association between the simulations and the measurements was calculated using a linear regression model (r^2). A *t*-test was used to assess the significance of the r^2 value.

3. Results

3.1 Model Evaluation Using Texture-Based or Machine Learning–Derived Porosity

The evaluation of the four models across the five datasets is illustrated in the heatmaps and summary plots (Fig. 1-6). Comparison of the results when soil porosity was estimated by (i) the TB approach, and (ii) the ML approach demonstrated that replacing TB- with ML-derived porosity generally improved model performance, reducing RMSE and increasing r^2 in most cases, although the magnitude and consistency of improvements varied across models and sites. The changes are most pronounced in the Bertagni and Ehhalt models and generally more modest in Morfopoulos and Smith–Downey.

The Bertagni model showed clear improvement when ML-derived porosity was used. The average RMSE decreased from 79.4 % with TB porosity to 56.7 % with ML porosity, while the average r^2

https://doi.org/10.5194/egusphere-2026-1312
Preprint. Discussion started: 23 March 2026
© Author(s) 2026. CC BY 4.0 License.

462 decreased slightly from 0.43 to 0.40. A standout performance gain occurred at the site described by
463 Lallo et al. (2008), where the RMSE was reduced significantly from 87.1% to 37.6% and r^2 rose from
464 0.38 to 0.65. The greatest gains occurred at the sites described by Meredith et al. (2017) and Cowan
465 et al. (2025; Forest), where ML porosity produced substantially lower RMSE values and higher r^2.
466 Bartyzel et al. (2013) showed improvement in RMSE (from 84.5% to 72.5%) while at the Cowan et al.
467 (2025; Grassland) site, the simulations showed an increase in RMSE (from 67.7% to 77.2%). The
468 average *p*-value increased from 0.04 to 0.25, suggesting weaker statistical significance.

469 The Morfopoulos model produced mixed results. On average, the value of RMSE increased from 81.9%
470 to 85.9%, driven by higher errors at Cowan et al. (2025; Grassland) (from 164.7 % to 257.6 %) and
471 Meredith et al. (2017) (from 31.7 % to 46.5 %). However, performance improved notably for Cowan et
472 al. (2025; Forest) (RMSE reduced from 75.5 % to 50.3 %), Bartyzel et al. (2013) (from 64.9 % to 47.0
473 %), and Lallo et al. (2008) (from 72.6% to 28.2%). Despite the increase in average RMSE, r^2 improved
474 from 0.58 to 0.62, indicating better fit between model and observations at several sites. The average
475 *p*-value increased slightly from 0.00 to 0.03.

476 The Ehhalt model largely benefited from using ML-derived porosity. The average RMSE decreased from
477 69.5 % to 50.9 %, and the average r^2 increased from 0.52 to 0.63, showing notable overall gains in both
478 accuracy and fit. At the Lallo et al. (2008) site, RMSE was nearly halved (85.9% to 49.3%) and r^2
479 improved from 0.43 to 0.78. At Meredith et al. (2017), model–data correspondence improved
480 substantially (RMSE reduced from 52.6% to 18.2%), while, at the Bartyzel et al. (2013) site, the RMSE
481 value increased slightly from 70.2% to 73.3%. The average *p*-value rose from 0.00 to 0.48, indicating
482 weaker statistical significance.

483 The Smith–Downey model showed moderate overall improvement with ML porosity. The average
484 RMSE decreased slightly from 84.2% to 79.4%, while the average r^2 remained unchanged at 0.58.
485 Improvements in RMSE were evident for Cowan et al. (2025; Forest) (80.2% to 70.3%), Meredith et al.
486 (2017), and Bartyzel et al. (2013) (41.8% to 33.4%), Bartyzel et al. (2013) (66.3% to 54.6%), and Lallo

https://doi.org/10.5194/egusphere-2026-1312
Preprint. Discussion started: 23 March 2026
© Author(s) 2026. CC BY 4.0 License.

et al. (2008) (76.1% to 54.8%). Cowan et al. (2025; Grassland) exhibited a sharp increase in error (156.7% to 185.7%). The average *p*-value increased from 0.00 to 0.11.

https://doi.org/10.5194/egusphere-2026-1312
Preprint. Discussion started: 23 March 2026
© Author(s) 2026. CC BY 4.0 License.

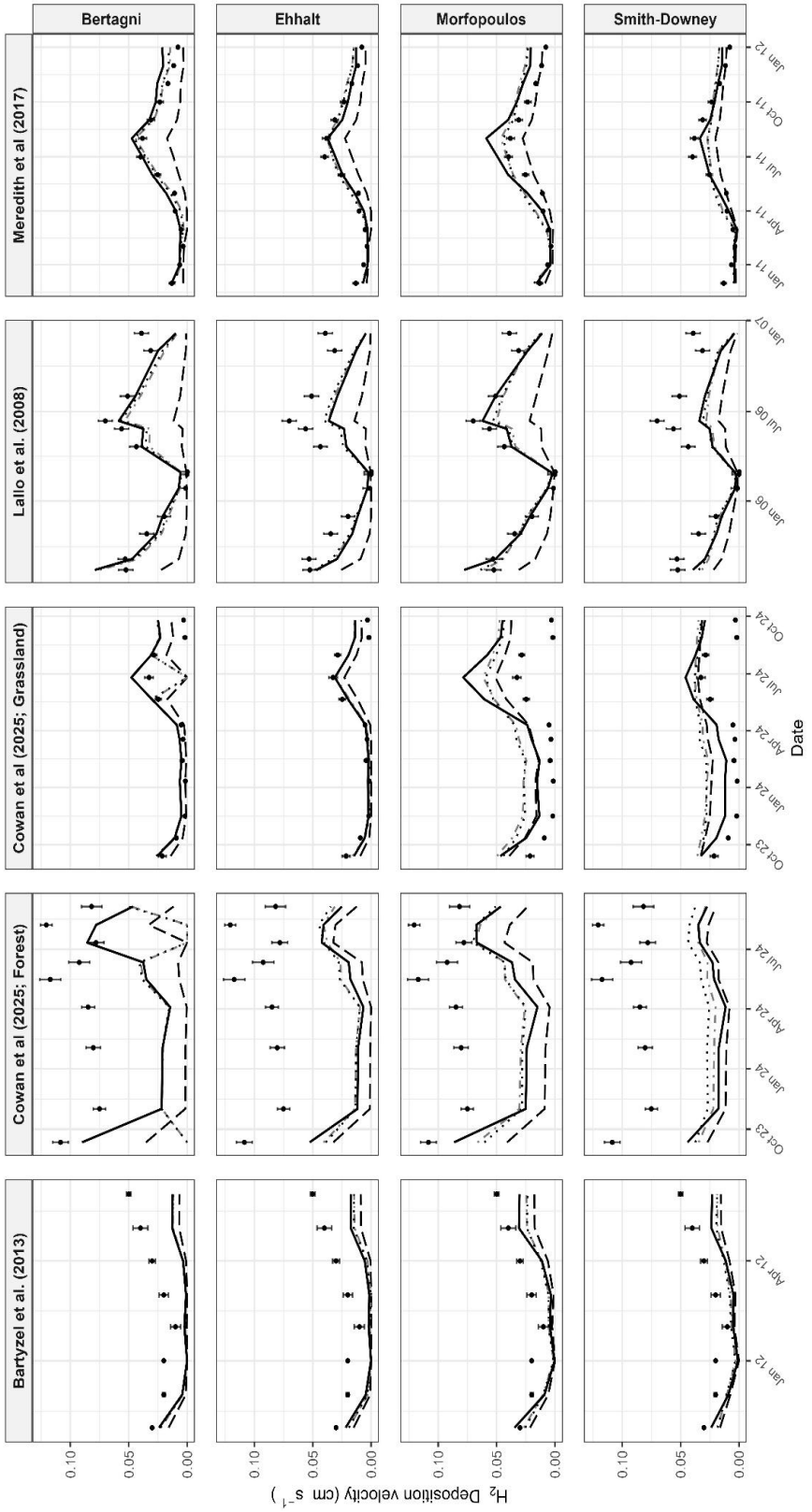

Figure 1 Comparison of measured monthly H_2 deposition velocity with simulations from four different models. Dashed lines represent the original model output, dot-dashed lines represent soil porosity estimated from machine learning (ML) approach, solid lines indicate model outputs incorporating coupled climate-carbon microbial activity rate modifier (m_{CCMAC}),dotted line indicates model outputs incorporating carbon-based microbial activity rate modifier (m_{CMAC}), and points represent the field data. Monthly H_2 deposition velocity is compared against simulations from the Bertagni (Bertagni et al., 2021), Morfopoulos (Morfopoulos et al., 2012), Ehhalt (Ehhalt and Rohrer, 2013), and Smith-Downey (Smith-Downey et al., 2007) models. Data were collected from a garden meadow with sandy clay loam soils (Bartyzel et al., 2013), a grassland with clay soils (Cowan et al., 2025; Grassland), a forest with sandy clay loam soils (Cowan et al., 2025; Forest), a forest with sand loam soils (Lallo et al., 2008) and Harvard Forest with sandy loam soils (Meredith et al., 2017).

https://doi.org/10.5194/egusphere-2026-1312
Preprint. Discussion started: 23 March 2026
© Author(s) 2026. CC BY 4.0 License.

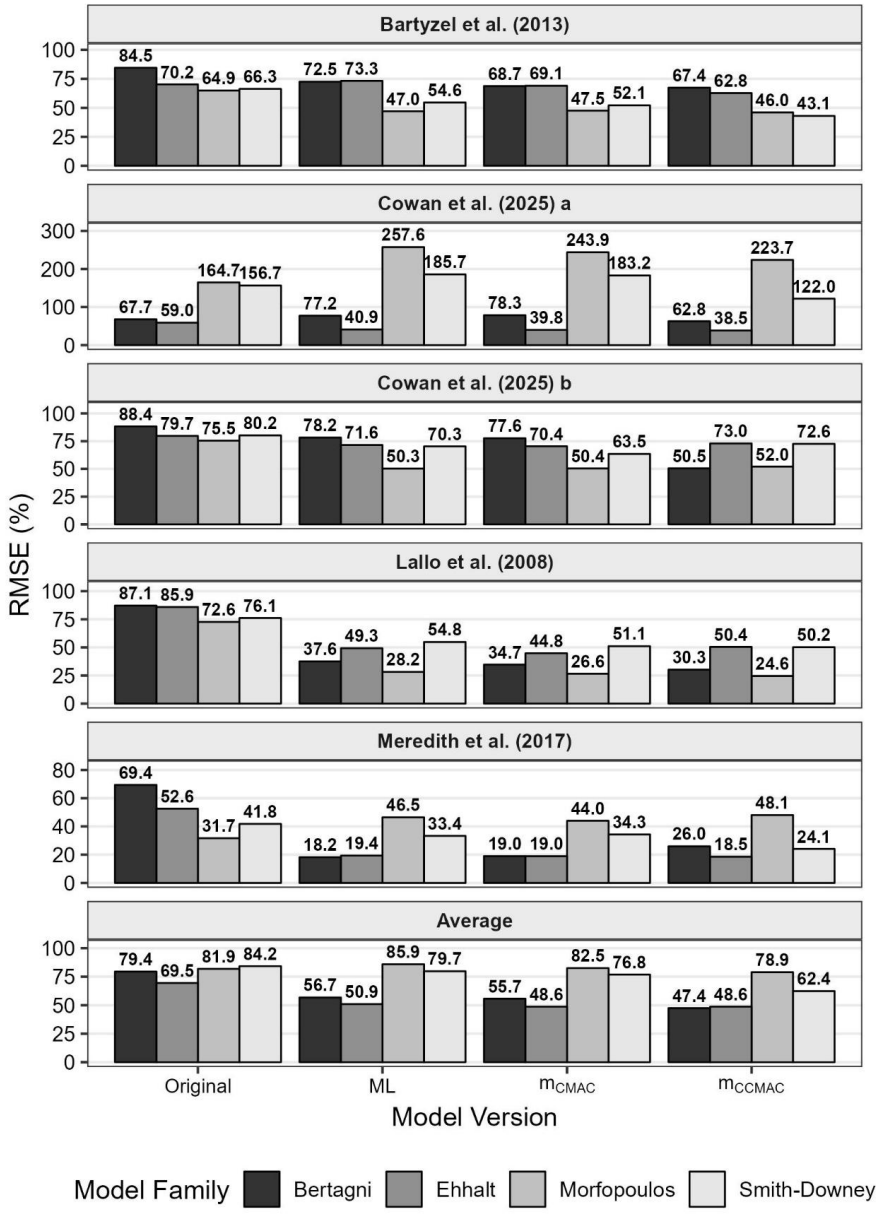

Figure 2: Comparison of model performance metrics (RMSE %) across different simulations from the Bertagni (Bertagni et al., 2021), Morfopoulos (Morfopoulos et al., 2012), Ehhalt (Ehhalt and Rohrer, 2013), and Smith-Downey (Smith-Downey et al., 2007) models. Original represent the original model output, ML represent soil porosity estimated from machine learning approach, m_{CMAC} indicate model outputs incorporating carbon-based microbial activity rate modifier, and m_{CCMAC} represent incorporating coupled climate-carbon microbial activity rate modifier.

https://doi.org/10.5194/egusphere-2026-1312
Preprint. Discussion started: 23 March 2026
© Author(s) 2026. CC BY 4.0 License.

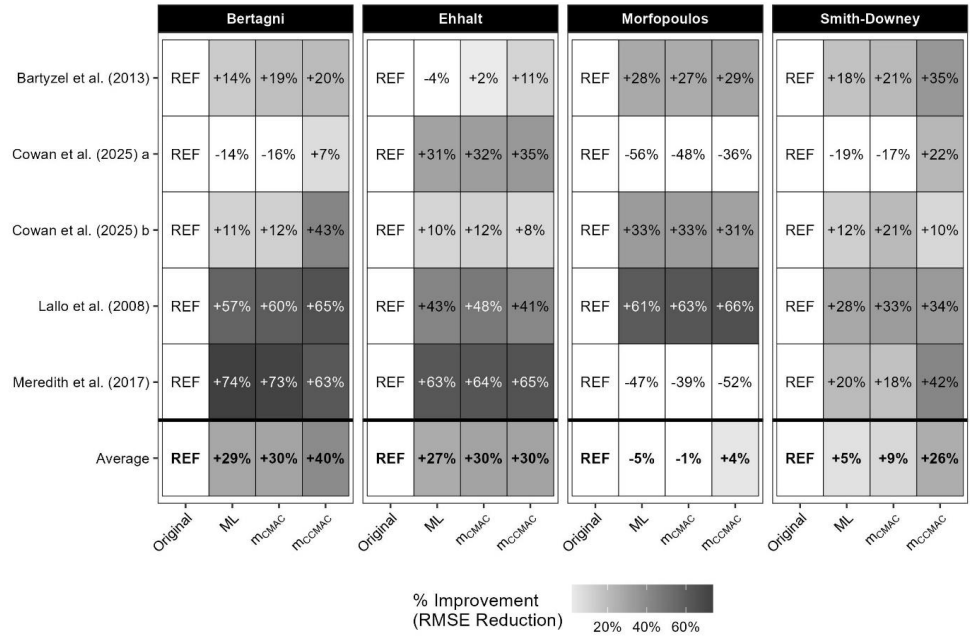

Figure 3: Heatmap showing the percentage improvement in Root Mean Square Error (RMSE) across various models. Cell values indicate the percentage reduction in RMSE relative to the "Original" version (REF); positive percentages denote increased model accuracy. The intensity of the grey scale corresponds to the magnitude of improvement. Original represent the original model output, ML represent soil porosity estimated from machine learning approach, m_{CMAC} indicate model outputs incorporating carbon-based microbial activity rate modifier, and m_{CCMAC} represents incorporating coupled climate-carbon microbial activity rate modifier.

https://doi.org/10.5194/egusphere-2026-1312
Preprint. Discussion started: 23 March 2026
© Author(s) 2026. CC BY 4.0 License.

519

520

521

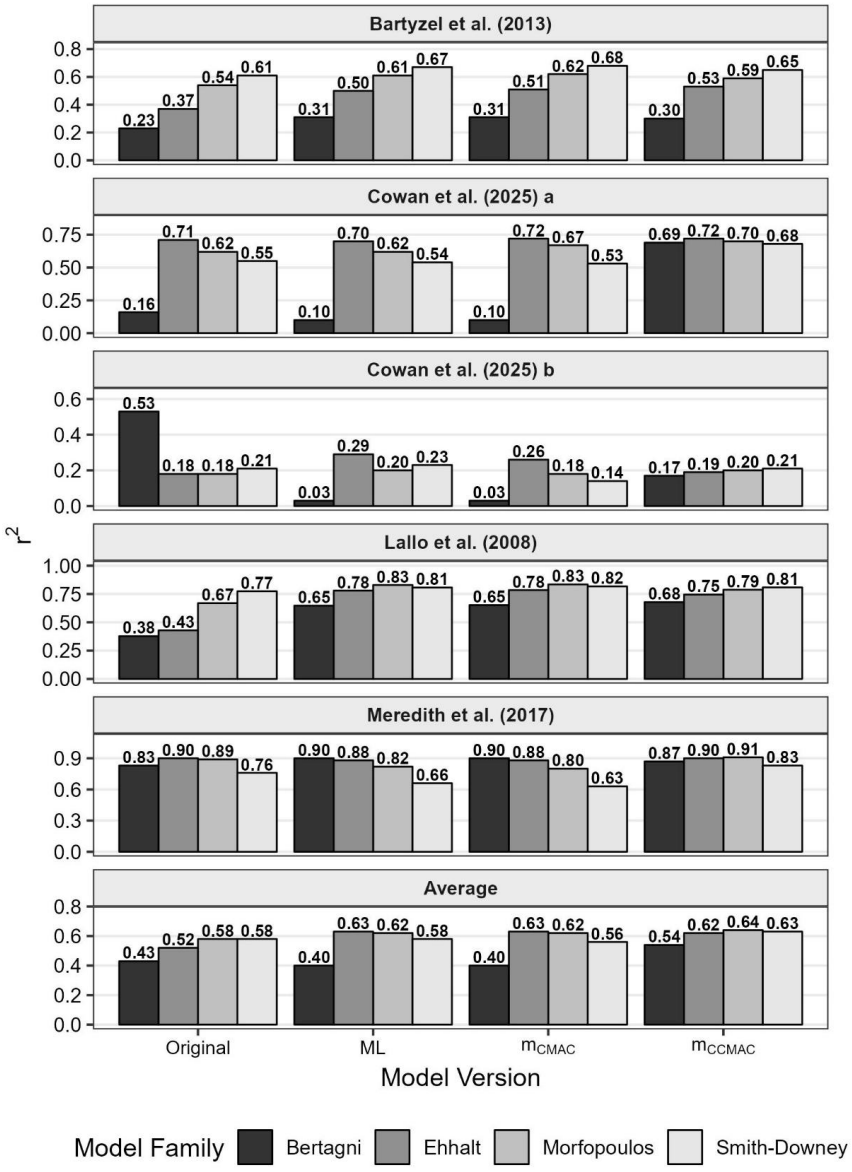

522

523 *Figure 4: Comparison of model performance metrics (r^2) across different simulations from the Bertagni (Bertagni et al.,*
524 *2021), Morfopoulos (Morfopoulos et al., 2012), Ehhalt (Ehhalt and Rohrer, 2013), and Smith-Downey (Smith-Downey et*
525 *al., 2007) models. Original represent the original model output, ML represent soil porosity estimated from machine*
526 *learning approach, m_{CMAC} indicate model outputs incorporating carbon-based microbial activity rate modifier, and*
527 *m_{CCMAC} represents incorporating coupled climate-carbon microbial activity rate modifier.*

https://doi.org/10.5194/egusphere-2026-1312
Preprint. Discussion started: 23 March 2026
© Author(s) 2026. CC BY 4.0 License.

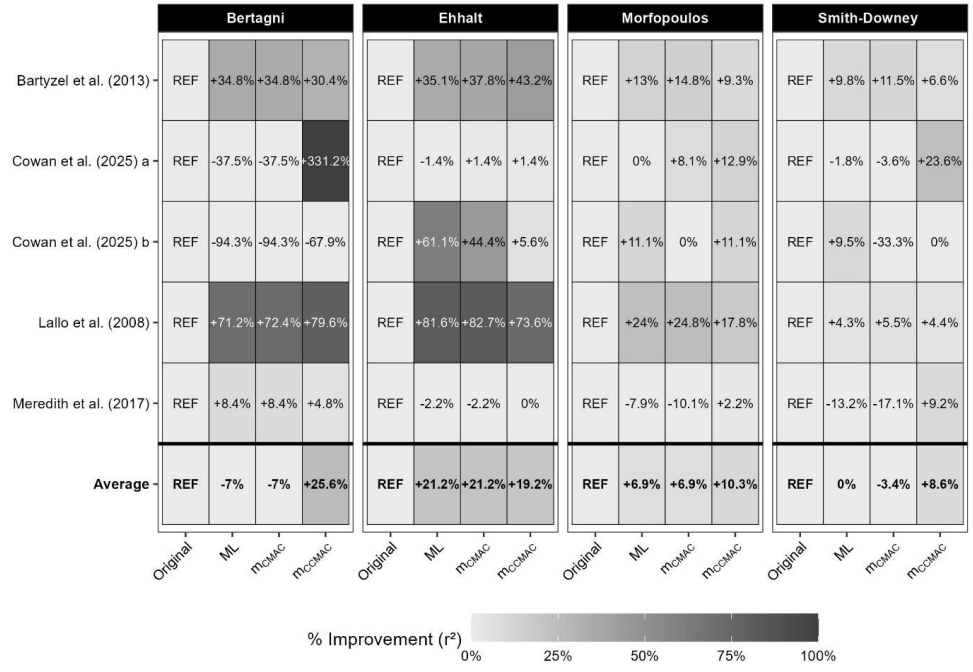

Figure 5: Relative Improvement in Model Performance (r^2) across study sites. Cell values indicate the percentage increase in r^2 relative to the "Original" version (REF); positive percentages denote increased model accuracy. The intensity of the grey scale corresponds to the magnitude of improvement. Original represent the original model output, ML represent soil porosity estimated from machine learning approach, m_{CMAC} indicate model outputs incorporating carbon-based microbial activity rate modifier, and m_{CCMAC} represents incorporating coupled climate-carbon microbial activity rate modifier.

https://doi.org/10.5194/egusphere-2026-1312
Preprint. Discussion started: 23 March 2026
© Author(s) 2026. CC BY 4.0 License.

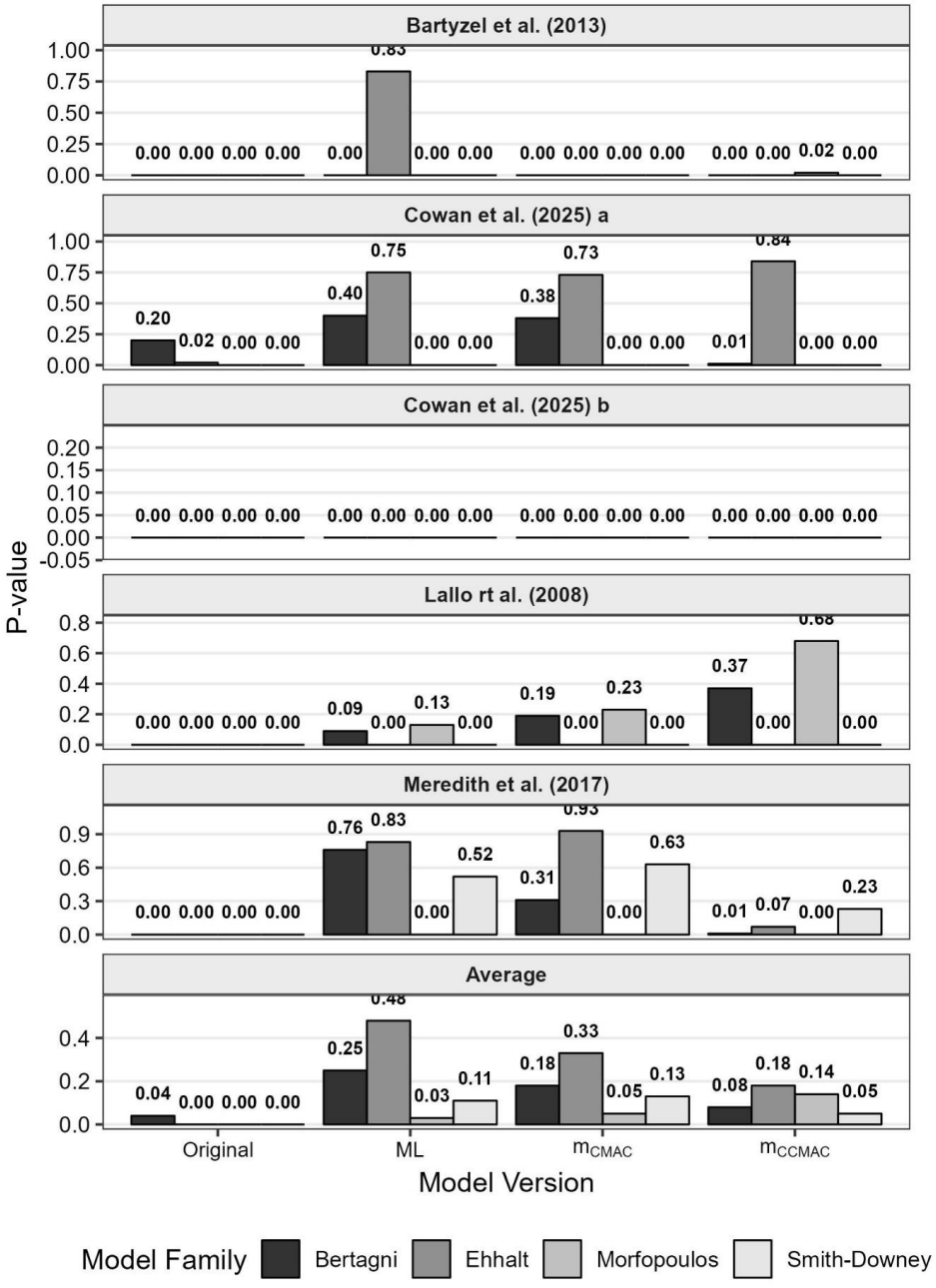

Figure 6: Comparison of p-values of t-test across different simulations from the Bertagni (Bertagni et al., 2021), Morfopoulos (Morfopoulos et al., 2012), Ehhalt (Ehhalt and Rohrer, 2013), and Smith-Downey (Smith-Downey et al., 2007) models. Original represent the original model output, ML represent soil porosity estimated from machine learning approach, m_{CMAC} indicate model outputs incorporating carbon-based microbial activity rate modifier, and m_{CCMAC} represents incorporating coupled climate-carbon microbial activity rate modifier.

https://doi.org/10.5194/egusphere-2026-1312
Preprint. Discussion started: 23 March 2026
© Author(s) 2026. CC BY 4.0 License.

3.2 Model Evaluation Using Carbon-Based Microbial Activity Rate Modifier

The evaluation of the four models across the five datasets is illustrated in the heatmaps and summary plots (Fig. 1-6). Overall, integrating the carbon-based microbial activity rate modifier (m_{CMAC}) into the H_2 uptake models, referred to in the figures as "Original + m_{CMAC}", led to modest but generally consistent improvements across most models. These improvements were primarily reflected in small reductions in prediction error (RMSE) and marginal changes in explanatory power (r^2). Among the four models, the Bertagni and Smith–Downey models showed the clearest overall reductions in RMSE, while the Ehhalt and Morfopoulos models exhibited smaller and dataset-dependent responses.

In the Bertagni model, inclusion of m_{CMAC} resulted in minor, but consistent, changes in model accuracy. The average RMSE decreased from 56.7% (with ML porosity) to 55.7%. Dataset-level responses were mixed, with reductions in RMSE for Lallo et al. (2008) (from 37.6% to 34.7%) and Bartyzel et al. (2013) (from 72.5% to 68.7%), while a slight increase was observed for Meredith et al. (2017) (from 18.2% to 19.0%). The average r^2 showed a small increase from 0.40 to 0.43, suggesting that the explanatory power of the model improved slightly. Average *p*-values also decreased from 0.25 to 0.18, indicating a modest improvement in statistical performance.

The Morfopoulos model exhibited mixed improvements when m_{CMAC} was included. On average, RMSE decreased from 85.9% to 82.5%. The most pronounced improvement occurred for Lallo et al. (2008), where RMSE declined from 28.2% to 26.6%. Explanatory power showed a slight increase, with average r^2 rising from 0.62 to 0.63. However, at the Cowan et al. (2025; Grassland) site, the RMSE value remained high, only slightly decreasing from 257.6% to 243.9%. Average *p*-values increased from 0.03 to 0.05, indicating a slight reduction in statistical significance.

In the Ehhalt model, changes associated with the inclusion of m_{CMAC} were minimal. The average RMSE decreased slightly from 50.9% to 48.6%, indicating marginal gains in predictive accuracy. Similarly, the mean r^2 remained unchanged at 0.63. While some datasets showed small improvements (e.g. for Lallo et al. (2008), RMSE fell from 49.3% to 44.8%), others exhibited negligible changes, such as Meredith

https://doi.org/10.5194/egusphere-2026-1312
Preprint. Discussion started: 23 March 2026
© Author(s) 2026. CC BY 4.0 License.

et al. (2017) where RMSE shifted from 19.4% to 19.0%. Average *p*-values decreased from 0.48 to 0.33, suggesting a small shift in statistical performance.

The Smith–Downey model showed the most consistent improvement across all datasets. The average RMSE decreased from 79.7% to 76.8%, reflecting an overall enhancement in predictive performance. Substantial reductions were observed for Lallo et al. (2008) (from 54.8% to 51.1%) and Cowan et al. (2025; Forest) (from 70.3% to 63.5%). Notably, at the Bartyzel et al. (2013) site, RMSE improved from 54.6% to 52.1%. However, average r^2 declined from 0.58 to 0.56, indicating a slight reduction in explanatory power despite lower errors. Average *p*-values increased from 0.11 to 0.13, suggesting stable statistical performance.

Across all four models, the inclusion of m_{CMAC} generally led to small reductions in RMSE, indicating modest improvements in predictive accuracy. The Bertagni and Smith–Downey models showed the clearest benefits in terms of average error reduction, whereas the Ehhalt and Morfopoulos models exhibited only marginal overall changes.

3.2 Model Evaluation Using Coupled Climate-Carbon Modifier

The evaluation of the four models across the five datasets is illustrated in the heatmaps and summary plots (Fig. 1-6). Overall, integrating coupled climate-carbon microbial activity rate modifier (m_{CCMAC}) into the H_2 uptake models substantially enhanced performance across most models. Improvements were generally reflected in higher explanatory power (r^2) and reduced prediction error (RMSE). Among the four models, the Bertagni, Morfopoulos and Smith–Downey models showed the most pronounced gains, while the Ehhalt model demonstrated more moderate improvements.

In the Bertagni model, the inclusion of m_{CCMAC} led to clear improvements in model accuracy across most datasets. The average RMSE decreased from 56.7% (ML-baseline) to 47.4%, indicating a notable improvement in alignment with observed field data. A striking improvement occurred for the Lallo et al. (2008) dataset, where RMSE dropped from 37.6% to 27.5%, and for Cowan et al. (2025; Grassland),

https://doi.org/10.5194/egusphere-2026-1312
Preprint. Discussion started: 23 March 2026
© Author(s) 2026. CC BY 4.0 License.

where it fell from 77.2% to 38.2%. Similarly, average r^2 increased from 0.40 to 0.58, representing a 25.6% improvement over the original model. Particularly strong gains in r^2 were observed for Cowan et al. (2025; Grassland) (from 0.10 to 0.70) and Cowan et al. (2025; Forest) (from 0.03 to 0.22). The average *p*-value decreased from 0.25 to 0.10, suggesting a significant improvement in the statistical reliability of the model fit.

The Morfopoulos model exhibited substantial improvements after incorporating m_{CCMAC}. On average, the RMSE declined from 85.9% to 71.3%, indicating a major reduction in prediction error. The largest improvement was again evident for Cowan et al. (2025; Forest), where RMSE decreased from 257.6% to 150.8%, and for Lallo et al. (2008), which achieved the lowest overall error at 24.6%. The r^2 also increased from 0.62 to 0.65, showing a general enhancement in model fit across sites. Notably, at the Meredith et al. (2017) site, r^2 increased from 0.82 to 0.91. The average *p*-value decreased from 0.05 to 0.02, confirming that the model was highly responsive to the addition of m_{CCMAC}.

In the Ehhalt model, changes were smaller and less consistent. The average RMSE showed only a slight decrease, from 50.9% to 48.2%, suggesting minimal overall effect on prediction accuracy. The mean r^2 decreased slightly from 0.63 to 0.59, indicating no clear improvement in explanatory capacity. The average *p*-value improved significantly, decreasing from 0.48 to 0.23. Overall, the Ehhalt model exhibited marginal benefits from incorporating microbial effects, with changes being small and site-dependent.

The Smith–Downey model showed notable and consistent improvement across most datasets after adding m_{CCMAC}. The average RMSE decreased from 79.7% to 65.4%, reflecting a considerable enhancement in predictive performance. Cowan et al. (2025; Grassland) showed the strongest response, with RMSE reducing from 185.7% to 122.0%, while Lallo et al. (2008) saw a reduction to 41.3%. The average r^2 increased from 0.58 to 0.63, a +8.6% improvement over the original model. The most substantial gains were seen in Meredith et al. (2017), where r^2 rose from 0.66 to 0.83. The

https://doi.org/10.5194/egusphere-2026-1312
Preprint. Discussion started: 23 March 2026
© Author(s) 2026. CC BY 4.0 License.

average *p*-value decreased from 0.11 to 0.06, highlighting that the model benefited significantly from coupled microbial integration.

Across all four models, the inclusion of the coupled climate-carbon microbial activity rate modifier (m_{CCMAC}) generally greatly improved model performance. The Bertagni, Morfopoulos and Smith–Downey models exhibited clear reductions in RMSE and notable increases in r^2, demonstrating stronger predictive capability and more robust fit to field observations. In contrast, the Ehhalt model showed limited sensitivity to this specific microbial enhancement, with only minor changes observed in performance metrics.

4. Discussion

Our study introduces a new framework for incorporating microbial activity into soil H_2 uptake models. The carbon-based microbial activity rate modifier (m_{CMAC}) uses the overall decomposability of SOC as a proxy for potential microbial activity, using the size and specific rate constants for decomposition of the different soil C pools to estimate overall SOC decomposability. Crucially, when environmental factors are coupled directly into the calculation (m_{CCMAC}), the results are substantially improved compared to the uncoupled version (m_{CMAC}). This biological refinement, complemented by the incorporation of ML-derived soil porosity, significantly strengthened overall model performance.

4.1 The Physical Constraint: Influence of Machine Learning-Derived Porosity on Gas Diffusion

A comparison of model outputs using ML-derived porosity with those using particle ratio-derived porosity shows that ML-based porosity generally enhanced model performance across the datasets. This improvement was most pronounced in the Bertagni and Ehhalt formulations. Conversely, the Morfopoulos model exhibited mixed performance trends, while the predictive metrics for the Smith–Downey model demonstrated only marginal differences between the two porosity approaches.

https://doi.org/10.5194/egusphere-2026-1312
Preprint. Discussion started: 23 March 2026
© Author(s) 2026. CC BY 4.0 License.

It is important to note that soil H_2 uptake is mainly a diffusion-controlled process. Therefore, when the porosity data obtained from ML were used, the results were improved. The traditional particle ratio method assumes that porosity is controlled mainly by soil texture fractions (sand, silt, and clay) and overlooks important influences, such as soil structure (Totsche et al., 2018; Young and Crawford, 2004), land use and management practices (Bronick and Lal, 2005; Strudley et al., 2008), and compaction effects (Schjønning et al., 2015). These factors can significantly affect pore connectivity, gas diffusion and microbial habitats. In contrast, the ML approach integrates these complex relationships through tree-based ensemble models, such as Random Forest and Gradient Boosting (Hengl et al. 2017). Using a large global soil profile database that includes information on texture, organic matter, topography and climate, it produces spatially detailed and realistic porosity estimates that provide better inputs for H_2 uptake models.

The different responses of the four models to ML-derived porosity can be explained by how each model represents soil diffusivity and the role that porosity plays within its structure. The observed significant improvement in the performance of both the Bertagni and Ehhalt models when incorporating ML-derived porosity is mechanistically linked to their structure. In the Bertagni model, diffusivity is calculated through a direct porosity formulation, which makes it highly sensitive to improved porosity inputs. The Ehhalt model also relies on a classical diffusion framework in which air-filled porosity strongly affects gas transport; therefore, the more realistic ML-derived porosity leads to large reductions in RMSE and clear improvements in r^2 across sites.

In contrast, the Morfopoulos and Smith–Downey models use porosity in a less direct way and depend on texture-based parameters. Because porosity affects these models both explicitly (through diffusion) and indirectly (through texture-related calibration terms), the benefit of switching to ML porosity is less predictable. At sites where ML porosity matches the real soil structure well (e.g. Lallo et al., 2008), the models perform better, but at other sites the mismatch between ML porosity and the models' texture-sensitive components leads to higher RMSE, even when r^2 improves. These models rely more

https://doi.org/10.5194/egusphere-2026-1312
Preprint. Discussion started: 23 March 2026
© Author(s) 2026. CC BY 4.0 License.

on texture classification than on absolute porosity values, which limits their ability to take full advantage of high-resolution ML inputs. As a result, improvements in diffusivity do not always lead to better flux predictions. This is evident at the Cowan et al. (2025; Grassland) site, where field reports indicated that H_2 uptake was primarily diffusion-driven. Cowan et al. (2025) noted that a simple regression using only soil moisture and temperature yielded an $r^2 = 0.60$ for the grassland, compared to only 0.14 for the forest site. The superior performance of the Bertagni and Ehhalt models when integrated with ML-derived porosity aligns with these observations, confirming that capturing the physical diffusion path is critical in this grassland site.

Overall, the results highlight that the choice of porosity parameterization is not a technical detail but a key determinant of model accuracy. Incorporating ML-derived soil information provides a more realistic representation of the soil physical environment and offers a pathway towards improved prediction of H_2 deposition processes in global atmospheric models.

4.2. Performance of Models with Microbial Rate Modifier Incorporation

The superior performance of m_{CCMAC} stems from substrate-specific sensitivity and its ability to capture the dynamic interplay between carbon quality and climate. While m_{CMAC} treats soil moisture and temperature modifiers as a simple linear scalar external to the carbon summation, m_{CCMAC} integrates these modifiers directly inside the exponential term ($C_{\mathrm{pool}} \times 1 - e^{-k_{\mathrm{pool}} \times m_{\mathrm{T}} \times m_{\mathrm{M}}}$). Because the carbon mass (C_{pool}) and rate constants (k_{pool}) vary significantly across the four pools, placing the environmental modifiers inside the exponent fundamentally changes the relative weighting of each pool during the calculation. As illustrated in Fig. 7, where individual pools were fixed at a constant mass ($C_{\mathrm{pool}} = 25$), different carbon pools exhibit distinct sensitivities to moisture and temperature. This mathematical coupling ensures that environmental fluctuations activate slow-turnover pools (e.g. HUM) with a kinetic response that differs from fast-turnover pools (e.g. DPM). This divergence is primarily driven by the specific rate constant of each pool; the most labile fraction (DPM, $k = 10\ y^{-1}$) shows the greatest departure from the climate baseline, while the most stable fraction

https://doi.org/10.5194/egusphere-2026-1312
Preprint. Discussion started: 23 March 2026
© Author(s) 2026. CC BY 4.0 License.

(HUM, $k = 0.02\ y^{-1}$) remains closest to it. By capturing these coupled kinetics, m_{CCMAC} performs better than m_{CMAC}, simulating microbial activity that is sensitive to both SOC quality and localized weather conditions.

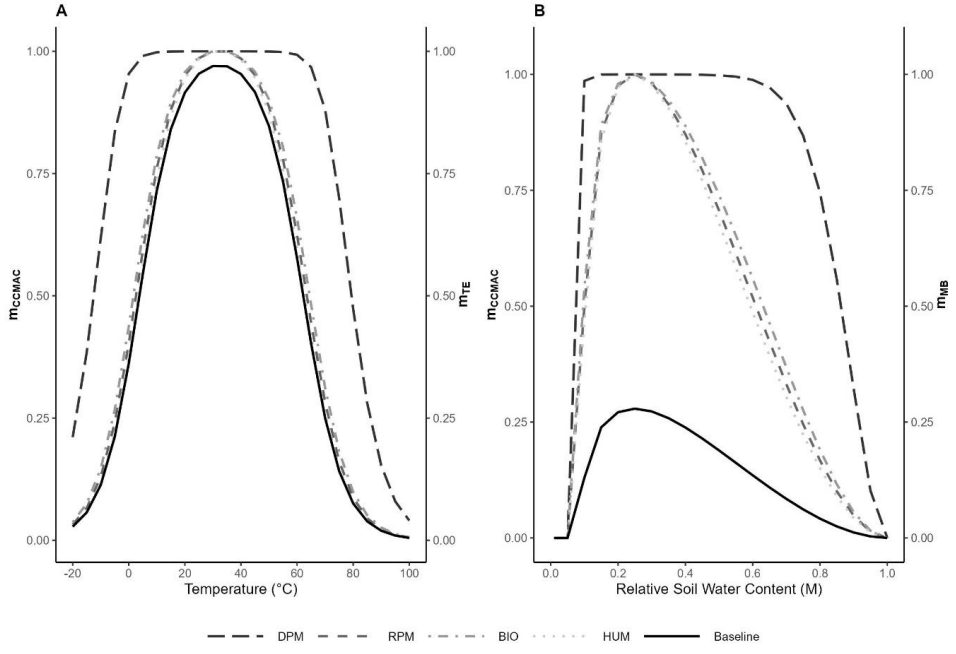

Figure 7: Sensitivity of SOC pools (DPM, RPM, BIO, and HUM) on temperature and moisture responses of the coupled climate-carbon modifier (m_{CCMAC}). A) thermal sensitivity of microbial activity when individual carbon pools are isolated at a constant mass of 25 t ha $^{-1}$ while maintaining other pools at zero ($m_{M,B=0.8}$). The solid line represents the temperature rate modifier ($m_{T,E}$) by Ehhalt et al. (2013) serving as the baseline for comparison. B) soil moisture sensitivity of microbial activity when individual carbon pools are isolated at a constant mass of 25 t ha $^{-1}$ while maintaining other pools at zero. The solid line represents the moisture rate modifier ($m_{M,B}$) serving as the baseline for comparison (soil temperature=20 °C, $\bar{s}_{ws} = 0.09$ and $\bar{s}_{opt} = 1$).

The potential influence of SOC on H_2 dynamics has been recognized in earlier studies. Notably, Conrad and Seiler (1985) observed a positive correlation between H_2 deposition velocities and SOC content. Building on this, Lallo et al. (2008) demonstrated higher deposition velocities on organic forest floors compared to mineral soils, although the specific influence of C versus porosity remained ambiguous. Further strengthening the link, Khdhiri et al. (2015) established a linear relationship between total organic C and H_2 uptake in soils. H_2 oxidizing microbes are involved in various C cycling processes (Piché-Choquette and Constant 2019). For instance, *Actinobacteria*, such as *Mycobacterium*

https://doi.org/10.5194/egusphere-2026-1312
Preprint. Discussion started: 23 March 2026
© Author(s) 2026. CC BY 4.0 License.

smegmatis, that can oxidize atmospheric H_2, are involved in SOC decomposition (King 2003). Furthermore, recent studies have shown that the exposure of soil to elevated H_2 concentrations representative of those found in nature (i.e., 10,000 ppmv) increases the total number of types of C substrates used, as well as the rate of their consumption within a defined time period (Khdhiri et al. 2017; Piché-Choquette et al. 2016). (Paul et al. 2016) also recognized the interconnectedness of H_2 oxidation and soil C dynamics. Therefore, a robust conceptual model for predicting H_2 oxidation in soils should encompass both H_2 uptake and the soil C activity.

The development of m_{CCMAC} was driven by the need to establish a more direct and mechanistic link between SOC and microbial activity, recognizing SOC as a primary driver of microbial processes alongside soil moisture and temperature. While other studies have attempted to incorporate SOC into models for estimating soil H_2 oxidation, these efforts have often relied on simplified representations. Morfopoulos et al. (2012) relied on net primary productivity as a proxy for potential microbial activity, leading to the exclusion of significant ecosystems, such as deserts which have low SOC contents, and not fully accounting for below ground microbial activity. Recent work by Jordaan et al. (2020) demonstrates the substantial H_2-oxidizing potential of desert soils, especially after rainfall events. Therefore, a comprehensive and accurate global soil H_2 uptake model must move beyond simplified approaches and consider the full spectrum of environmental heterogeneity, including the previously underestimated contribution of deserts. Paulot et al. (2021) incorporated SOC into their model by adding a constant term to the Ehhalt model, further assuming a Michaelis-Menten dependence of this constant on measured soil C content. While this approach yields geographically varying deposition patterns (faster in tropics and high latitudes, slower in arid regions), it fails to capture the dynamic interplay between SOC cycling and H_2 oxidation.

4.3 Estimating Soil Moisture Thresholds

The study also highlights sources of uncertainty, especially in the estimation of soil moisture thresholds, minimum ($\bar{s}_{\mathrm{ws}}$) and optimum ($\bar{s}_{\mathrm{opt}}$) soil moisture levels, used in calculating m_{CCMAC} and

https://doi.org/10.5194/egusphere-2026-1312
Preprint. Discussion started: 23 March 2026
© Author(s) 2026. CC BY 4.0 License.

within the Bertagni model. These thresholds are estimated solely from soil texture, following the same approach used to calculate total soil porosity (Campbell, 1974). However, relying only on soil texture overlooks other factors, such as soil structure, organic matter and compaction, which can strongly influence microbial activity.

This limitation helps explain the model's underestimation of H_2 uptake in both the grassland and forest sites measured by Cowan et al. (2025). In these datasets, the observed H_2 uptake peaked during dry summer periods, when soil moisture was low. The original Bertagni model predicted almost no microbial activity under these dry conditions, leading to an underestimation of H_2 uptake. After incorporating m_{CCMAC}, the model reproduced the observed uptake patterns more accurately. This improvement was due to the better estimation of $\bar{s}_{\mathrm{ws}}$ using PTFs (Eq. 25 and Eq. 26) within m_{CCMAC}, which provided a more realistic representation of soil moisture thresholds that control microbial processes. This shift is supported by the laboratory measurements from Reji et al. (2025), who found that $\bar{s}_{\mathrm{ws}}$ is unexpectedly low, with measurable H_2 oxidation occurring at water potentials between -70 and -100 MPa.

Overall, these findings suggest that estimating soil moisture thresholds from texture alone introduces significant uncertainty. Incorporating PTF-based estimates that account for broader soil physical and biological properties improves the accuracy of moisture-related parameters. By moving away from plant-centric thresholds toward thresholds that reflect the thermodynamic limits of specialized microbes, models can better simulate uptake in extreme environment.

Accurately determining $\bar{s}_{\mathrm{ws}}$ and $\bar{s}_{\mathrm{opt}}$ remains a key challenge, as these parameters are influenced by multiple factors beyond texture, including soil structure (Liu et al. 2022), electrical conductivity (Fu, Horton, and Heitman 2021), SOC content (Lal et al. 2018), temperature (Campbell and Norman 1998) and salinity (Morrissey et al. 2014). The results of this study show that estimating $\bar{s}_{\mathrm{ws}}$ and $\bar{s}_{\mathrm{opt}}$ using PTFs that incorporate both soil particle ratios and SOC content enhances model performance. In general, the threshold values derived from PTFs are lower than those estimated from texture-based

https://doi.org/10.5194/egusphere-2026-1312
Preprint. Discussion started: 23 March 2026
© Author(s) 2026. CC BY 4.0 License.

methods (Table 3), algins with laboratory measurement by Reji et al. (2025). This adjustment enables the model to better capture microbial activity under dry soil conditions, where measurable H_2 oxidation can still occur.

Overall, our findings indicate that PTF-based estimates of $\bar{s}_{\mathrm{ws}}$ and $\bar{s}_{\mathrm{opt}}$ enhance model performance by more accurately representing the hydrological limits relevant to microbial physiology. They also align with emerging evidence that microbial activity can continue at soil water potentials well below the traditional plant wilting point (Liang et al. 2022), a complexity not yet fully incorporated into most ecosystem models. Future laboratory studies that directly quantify H_2 uptake across a range of low-moisture conditions are critically needed. Such measurements would enable empirical calibration of PTF-derived thresholds and further improve the predictive accuracy of soil biogeochemical models under extreme moisture regimes.

4.4 Limitations and Future Research

While the inclusion of m_{CCMAC} improved model performance and biological realism, several limitations remain. Despite the inclusion of five diverse datasets, the evaluation still covers a relatively limited range of the Earth's ecosystems. Key regions, such as high-latitude permafrost soils or tropical wetlands, remain under-represented.

Microbial H_2 uptake remains active across extreme moisture gradients, which presents unique challenges for current modelling frameworks. At the dry end of the spectrum, microbial uptake persists at moisture levels far below the plant wilting point, a process that is currently not represented well in existing models. Conversely, uptake continues in saturated soils due to the unique physical properties of H_2. As the smallest molecule, H_2 diffuses effectively through thin water films and navigates through pockets of trapped air within the saturated soil matrix. Because these mechanisms differ significantly from transport in intermediate soil conditions, it is essential to expand our empirical understanding. Future research must prioritize the collection of data across both the very dry and the fully saturated ends of the soil moisture spectrum to improve the accuracy of environmental models.

https://doi.org/10.5194/egusphere-2026-1312
Preprint. Discussion started: 23 March 2026
© Author(s) 2026. CC BY 4.0 License.

5. Conclusion

This study provides a comprehensive evaluation of soil H_2 uptake models, demonstrating that the accuracy of global sink estimates depends on both physical parameters and mechanistically coupled biological drivers.

Our results confirm that ML-derived porosity significantly outperforms traditional texture-based methods. By capturing complex, non-linear relationships between soil structure, organic matter and management practices, the ML approach provides a more realistic physical "template" for gas diffusion. This was particularly evident in the Bertagni and Ehhalt models, where the transition to ML-based porosity led to a substantial reduction in RMSE and enhanced correlation with field observations.

Furthermore, this work establishes microbial activity as a primary regulator of soil H_2 dynamics. The transition from a carbon-based microbial activity rate modifier (m_{CMAC}) to a coupled climate-carbon modifier (m_{CCMAC}) proved essential for capturing the biological signal. By placing environmental modifiers inside the exponential term, the m_{CCMAC} framework accounts for the substrate-specific sensitivity of different carbon pools. Integrating m_{CCMAC} led to stronger model-data correspondence for the Bertagni, Morfopoulos, and Smith–Downey models. In contrast, the Ehhalt model's performance was relatively unaffected, suggesting that its structure is less responsive to this specific adjustment.

By addressing the missing component of microbial dynamics in existing H_2 uptake models, this work underscores the necessity of integrating biotic factors into global frameworks. The m_{CCMAC} modifier provides a mechanistically grounded and ecologically representative pathway for predicting atmospheric H_2 cycling, offering more robust projections of the soil sink under changing global environmental conditions.

Acknowledgements:

https://doi.org/10.5194/egusphere-2026-1312
Preprint. Discussion started: 23 March 2026
© Author(s) 2026. CC BY 4.0 License.

The authors acknowledge support from the Natural Environment Research Council (NERC) grant no. NE/X013464/1. Climate data were obtained from the NASA Langley Research Center (LaRC) POWER Project funded through the NASA Earth Science/Applied Science Program. We acknowledge the use of model input data from the TRENDYv10 project (LPJ NPP, provided by B. Poulter), LPJ-GUESS simulations from the Karlsruhe Institute of Technology (soil temperature and moisture, provided by P. Anthoni), and ERA5 reanalysis data (climate variables, provided by the European Centre for Medium-Range Weather Forecasts).

Author contributions:

SK performed the literature review, wrote the initial manuscript drafts, JS and SK developed the modelling framework, JS supervised the entire research process and provided overall project guidance. JD, JFD, and PS contributed to the critical review and editing of the manuscript.

Data availability:

The spreadsheet used to calculate the coupled climate-carbon microbial activity rate modifier (m_{CCMAC}) is based on the RothC model and is available at https://github.com/saeedkarbin/mCCMAC/blob/main/RothC-mCCMAC.xlsm .

References

Abdalla, M, A Hastings, M Helmy, A Prescher, B Osborne, G Lanigan, D Forristal, DİLEK Killi, P Maratha, and M Williams. 2014. 'Assessing the Combined Use of Reduced Tillage and Cover Crops for Mitigating Greenhouse Gas Emissions from Arable Ecosystem'. *Geoderma* 223:9–20.

Abegaz, Assefa, Leigh A. Winowiecki, Tor-G. Vågen, Simon Langan, and Jo U. Smith. 2016. 'Spatial and Temporal Dynamics of Soil Organic Carbon in Landscapes of the Upper Blue Nile Basin of the Ethiopian Highlands'. *Agriculture, Ecosystems & Environment* 218 (February):190–208. https://doi.org/10.1016/j.agee.2015.11.019.

Anthoni, P. 2021. 'LPJ-GUESS S0 Scenario Output: Soil Temperature an d Moisture'. Karlsruhe Institute of Technology (KIT). https://doi.org/Contact: peter.anthoni@kit.edu.

Bartyzel, J., J. M. Necki, D. Zieba, K. Rozanski, and M. Gasiorek. 2013. 'Uptake Of Atmospheric Hydrogen By Soils: A Case Study From Southern Poland'. *European Journal of Soil Science* 64 (5): 597–609. https://doi.org/10.1111/EJSS.12066.

https://doi.org/10.5194/egusphere-2026-1312
Preprint. Discussion started: 23 March 2026
© Author(s) 2026. CC BY 4.0 License.

Bastida, Felipe, David J. Eldridge, Carlos García, G. Kenny Png, Richard D. Bardgett, and Manuel Delgado-Baquerizo. 2021. 'Soil Microbial Diversity–Biomass Relationships Are Driven by Soil Carbon Content across Global Biomes'. *The ISME Journal* 15 (7): 2081–91. https://doi.org/10.1038/s41396-021-00906-0.

Bertagni, Matteo B., Fabien Paulot, and Amilcare Porporato. 2021. 'Moisture Fluctuations Modulate Abiotic and Biotic Limitations of H2 Soil Uptake'. *Global Biogeochemical Cycles* 35 (12). https://doi.org/10.1029/2021GB006987.

Bousquet, P., C. Yver, I. Pison, Y. S. Li, A. Fortems, D. Hauglustaine, S. Szopa, et al. 2011. 'A Three-Dimensional Synthesis Inversion of the Molecular Hydrogen Cycle: Sources and Sinks Budget and Implications for the Soil Uptake'. *Journal of Geophysical Research: Atmospheres* 116 (D1). https://doi.org/10.1029/2010JD014599.

Brand, A., A. Lilly, and J. Smith. 2020. 'A Simple Approach to Modelling the Soil Water Budget in Cool Temperate Mineral Topsoils'. *Environmental Modelling and Software* 127. https://doi.org/10.1016/j.envsoft.2020.104700.

Bronick, Carol Jean, and Rattan Lal. 2005. 'Soil Structure and Management: A Review'. *Geoderma* 124 (1–2): 3–22.

Buzzard, Vanessa, Dana Thorne, Juliana Gil-Loaiza, Alejandro Cueva, and Laura K. Meredith. 2022. 'Sensitivity of Soil Hydrogen Uptake to Natural and Managed Moisture Dynamics in a Semiarid Urban Ecosystem'. *PeerJ* 10 (March):e12966. https://doi.org/10.7717/PEERJ.12966/SUPP-11.

Campbell, Gaylon S. 1974. 'A Simple Method for Determining Unsaturated Conductivity from Moisture Retention Data'. *Soil Science* 117 (6): 311–14.

Campbell, Gaylon S., and J. M. Norman. 1998. 'An Introduction to Environmental'. *Biophysics*.

Conrad, Ralf, and Wolfgang Seiler. 1981. 'Decomposition of Atmospheric Hydrogen by Soil Microorganisms and Soil Enzymes'. *Soil Biology and Biochemistry* 13 (1): 43–49. https://doi.org/10.1016/0038-0717(81)90101-2.

Conrad, Ralf, and Wolfgang Seiler. 1985. 'Influence of Temperature, Moisture, and Organic Carbon on the Flux of H_2 and CO between Soil and Atmosphere: Field Studies in Subtropical Regions'. *Journal of Geophysical Research* 90 (D3): 5699. https://doi.org/10.1029/JD090iD03p05699.

Constant, Philippe, Laurier Poissant, and Richard Villemur. 2008. 'Isolation of Streptomyces Sp. PCB7, the First Microorganism Demonstrating High-Affinity Uptake of Tropospheric H2'. *The ISME Journal* 2 (10): 1066–76. https://doi.org/10.1038/ismej.2008.59.

Cowan, Nicholas, Toby Roberts, Mark Hanlon, Aurelia Bezanger, Galina Toteva, Alex Tweedie, Karen Yeung, et al. 2025. 'Quantifying the Soil Sink of Atmospheric Hydrogen: A Full Year of Field Measurements from Grassland and Forest Soils in the UK'. *Biogeosciences* 22 (13): 3449–61. https://doi.org/10.5194/bg-22-3449-2025.

Dingman, S Lawrence. 2015. *Physical Hydrology*. Waveland press.

Dondini, M., Giorgio Alberti, Gemini Delle Vedove, Maurizio Ventura, Giustino Tonon, M. Viger, Z. M. Harris, J. R. Jenkins, M. Richards, and M. Pogson. 2017. 'Evaluation of the ECOSSE Model to Predict Heterotrophic Soil Respiration by Direct Measurements'. *European Journal of Soil Science* 68 (3): 384–93.

Dondini, Marta, Edward O. Jones, Mark Richards, Mark Pogson, Rebecca L. Rowe, Aidan M. Keith, Mike P. Perks, Niall P. McNamara, Joanne U. Smith, and Pete Smith. 2015. 'Evaluation of the ECOSSE Model for Simulating Soil Carbon under Short Rotation Forestry Energy Crops in Britain'. *Gcb Bioenergy* 7 (3): 527–40.

Dondini, Marta, Mark IA Richards, Mark Pogson, Jon McCalmont, Julia Drewer, Rachel Marshall, Ross Morrison, Sirwan Yamulki, Zoe M. Harris, and Giorgio Alberti. 2016. 'Simulation of Greenhouse Gases Following Land-use Change to Bioenergy Crops Using the ECOSSE Model: A Comparison between Site Measurements and Model Predictions'. *Gcb Bioenergy* 8 (5): 925–40.

https://doi.org/10.5194/egusphere-2026-1312
Preprint. Discussion started: 23 March 2026
© Author(s) 2026. CC BY 4.0 License.

Dondini, Marta, Mark Richards, Mark Pogson, Edward O. Jones, Rebecca L. Rowe, Aidan M. Keith, Niall P. McNamara, Joanne U. Smith, and Pete Smith. 2016. 'Evaluation of the ECOSSE Model for Simulating Soil Organic Carbon under Miscanthus and Short Rotation Coppice-Willow Crops in Britain'. *GCB Bioenergy* 8 (4): 790–804. https://doi.org/10.1111/gcbb.12286.

Dong, Z., and D. B. Layzell. 2001. 'H2 Oxidation, O2 Uptake and CO2 Fixation in Hydrogen Treated Soils'. *Plant and Soil* 229 (1): 1–12. https://doi.org/10.1023/A:1004810017490/METRICS.

Drewer, Julia, Nicholas J. Cowan, Mark Hanlon, Toby Roberts, Saeed Karbin, Ruby Devlin, Rujuta Nalavade, Eiko Nemitz, Alex Tweedie, and Aurelia Bezanger. 2026. 'Characterizing Environmental Drivers of the Soil Hydrogen Sink Through Controlled Laboratory Experiments'. SSRN Scholarly Paper. Rochester, NY: Social Science Research Network. https://doi.org/10.2139/ssrn.6222017.

Ehhalt, D. H., and F. Rohrer. 2009. 'The Tropospheric Cycle of H_2 A Critical Review'. *Tellus B: Chemical and Physical Meteorology* 61 (3): 500. https://doi.org/10.1111/j.1600-0889.2009.00416.x.

Ehhalt, D. H., and F. Rohrer. 2011. 'The Dependence of Soil H_2 Uptake on Temperature and Moisture: A Reanalysis of Laboratory Data'. *Tellus B: Chemical and Physical Meteorology* 63 (5): 1040. https://doi.org/10.1111/j.1600-0889.2011.00581.x.

Ehhalt, Dieter H., and Franz Rohrer. 2013. 'Dry Deposition of Molecular Hydrogen in the Presence of H₂ Production'. *Tellus B: Chemical and Physical Meteorology* 65 (1): 20620. https://doi.org/10.3402/tellusb.v65i0.20620.

Ehhalt, Dieter, and Franz Rohrer. 2013. 'Deposition Velocity of H2: A New Algorithm for Its Dependence on Soil Moisture and Temperature'. *Tellus, Series B: Chemical and Physical Meteorology* 65 (1). https://doi.org/10.3402/tellusb.v65i0.19904.

FAO. 2017. *Unlocking the Potential of Soil Organic Carbon – Outcome Document of the Global Symposium on Soil Organic Carbon*. FAO ; https://openknowledge.fao.org/handle/20.500.14283/i7268en.

Fery, S, and J M Melillo. 2025. 'Barre Woods Soil Warming Experiment at Harvard Forest since 2001'. Harvard Forest Data Archive: HF018. https://doi.org/10.6073/pasta/8becbc2b5a15f37cddc94b332b65e78a.

Fu, Yongwei, Robert Horton, and Josh Heitman. 2021. 'Estimation of Soil Water Retention Curves from Soil Bulk Electrical Conductivity and Water Content Measurements'. *Soil and Tillage Research* 209 (May):104948. https://doi.org/10.1016/j.still.2021.104948.

Gottschalk, P., J. U. Smith, M. Wattenbach, J. Bellarby, E. Stehfest, N. Arnell, T. J. Osborn, C. Jones, and P. Smith. 2012. 'How Will Organic Carbon Stocks in Mineral Soils Evolve under Future Climate? Global Projections Using RothC for a Range of Climate Change Scenarios'. *Biogeosciences* 9 (8): 3151–71. https://doi.org/10.5194/bg-9-3151-2012.

Hengl, Tomislav, Jorge Mendes de Jesus, Gerard B. M. Heuvelink, Maria Ruiperez Gonzalez, Milan Kilibarda, Aleksandar Blagotić, Wei Shangguan, et al. 2017. 'SoilGrids250m: Global Gridded Soil Information Based on Machine Learning'. *PLOS ONE* 12 (2): e0169748. https://doi.org/10.1371/journal.pone.0169748.

Hersbach, H, B Bell, P Berrisford, G Biavati, and Horányi. 2023. 'ERA5 Monthly Averaged Data on Single Levels from 1940 to Present'. Copernicus Climate Change Service (C3S) Climate Data Store (CDS). https://doi.org/10.24381/cds.f17050d7.

Jordaan, Karen, Rachael Lappan, Xiyang Dong, Ian J. Aitkenhead, Sean K. Bay, Eleonora Chiri, Nimrod Wieler, et al. 2020. 'Hydrogen-Oxidizing Bacteria Are Abundant in Desert Soils and Strongly Stimulated by Hydration'. *mSystems* 5 (6). https://doi.org/10.1128/MSYSTEMS.01131-20.

Khdhiri, Mondher, Laura Hesse, Maria Elena Popa, Liliana Quiza, Isabelle Lalonde, Laura K. Meredith, Thomas Röckmann, and Philippe Constant. 2015. 'Soil Carbon Content and Relative Abundance of High Affinity H2-Oxidizing Bacteria Predict Atmospheric H2 Soil

https://doi.org/10.5194/egusphere-2026-1312
Preprint. Discussion started: 23 March 2026
© Author(s) 2026. CC BY 4.0 License.

Uptake Activity Better than Soil Microbial Community Composition'. *Soil Biology and Biochemistry* 85:1–9. https://doi.org/10.1016/j.soilbio.2015.02.030.

Khdhiri, Mondher, Sarah Piché-Choquette, Julien Tremblay, Susannah G. Tringe, and Philippe Constant. 2017. 'The Tale of a Neglected Energy Source: Elevated Hydrogen Exposure Affects Both Microbial Diversity and Function in Soil'. *Applied and Environmental Microbiology* 83 (11). https://doi.org/10.1128/AEM.00275-17.

King, Gary M. 2003. 'Contributions of Atmospheric CO and Hydrogen Uptake to Microbial Dynamics on Recent Hawaiian Volcanic Deposits'. *Applied and Environmental Microbiology* 69 (7): 4067–75. https://doi.org/10.1128/AEM.69.7.4067-4075.2003/FORMAT/EPUB.

Lal, Rattan, Pete Smith, Hermann F. Jungkunst, William J. Mitsch, Johannes Lehmann, P. K. Ramachandran Nair, Alex B. McBratney, et al. 2018. 'The Carbon Sequestration Potential of Terrestrial Ecosystems'. *Journal of Soil and Water Conservation* 73 (6): 145A-152A. https://doi.org/10.2489/jswc.73.6.145A.

Lallo, Marko, T. Aalto, T. Laurila, and J. Hatakka. 2008. 'Seasonal Variations in Hydrogen Deposition to Boreal Forest Soil in Southern Finland'. *Geophysical Research Letters* 35 (4). https://doi.org/10.1029/2007GL032357.

Liang, Junyi, Kangli Chen, Siqintana, Tianci Huo, Yaowen Zhang, Jingying Jing, and Wenting Feng. 2022. 'Towards Improved Modeling of SOC Decomposition: Soil Water Potential beyond the Wilting Point'. *Global Change Biology* 28 (11): 3665–73. https://doi.org/10.1111/gcb.16127.

Liu, Lin, Yili Lu, Yongwei Fu, Robert Horton, and Tusheng Ren. 2022. 'Estimating Soil Water Suction from Texture, Bulk Density and Electrical Resistivity'. *Geoderma* 409 (March):115630. https://doi.org/10.1016/j.geoderma.2021.115630.

Meredith, Laura K., Róisín Commane, Trevor F. Keenan, Stephen T. Klosterman, J. William Munger, Pamela H. Templer, Jianwu Tang, Steven C. Wofsy, and Ronald G. Prinn. 2017. 'Ecosystem Fluxes of Hydrogen in a Mid-Latitude Forest Driven by Soil Microorganisms and Plants'. *Global Change Biology* 23 (2). https://doi.org/10.1111/gcb.13463.

Meredith, Laura K., Deepa Rao, Tanja Bosak, Vanja Klepac-Ceraj, Kendall R. Tada, Colleen M. Hansel, Shuhei Ono, and Ronald G. Prinn. 2014. 'Consumption of Atmospheric Hydrogen during the Life Cycle of Soil-Dwelling Actinobacteria'. *Environmental Microbiology Reports* 6 (3): 226–38. https://doi.org/10.1111/1758-2229.12116/SUPPINFO.

Meredith, Laura, S Wofsy, and R Prinn. 2023. 'Fluxes of Molecular Hydrogen (H2) at Harvard Forest EMS Tower 2010-2012 (HF288)'. Harvard Forest Data Archive: HF288. https://doi.org/10.6073/pasta/132513a992c9f3e554ae4012175e5b0a.

Millington, R. J., and J. P. Quirk. 1961. 'Permeability of Porous Solids'. *Transactions of the Faraday Society* 57:1200. https://doi.org/10.1039/tf9615701200.

Morfopoulos, C., P. N. Foster, P. Friedlingstein, P. Bousquet, and I. C. Prentice. 2012. 'A Global Model for the Uptake of Atmospheric Hydrogen by Soils'. *Global Biogeochemical Cycles* 26 (3). https://doi.org/10.1029/2011GB004248.

Morrissey, Ember M., Jaimie L. Gillespie, Joseph C. Morina, and Rima B. Franklin. 2014. 'Salinity Affects Microbial Activity and Soil Organic Matter Content in Tidal Wetlands'. *Global Change Biology* 20 (4): 1351–62. https://doi.org/10.1111/gcb.12431.

Nachtergaele, Freddy, Harrij Van Velthuizen, Luc Verelst, Niels Batjes, Koos Dijkshoorn, Vincent van Engelen, Guenther Fischer, Arwyn Jones, Luca Montanarella, and Monica Petri. 2010. 'Harmonized World Soil Database'. In , 2010:34–37. International Union of Soil Sciences.

Ouyang, Zutao, Robert B. Jackson, Marielle Saunois, Josep G. Canadell, Yuanhong Zhao, Catherine Morfopoulos, Paul B. Krummel, et al. 2025. 'The Global Hydrogen Budget'. *Nature* 648 (8094): 616–24. https://doi.org/10.1038/s41586-025-09806-1.

Paul, Alexia, Christine Hatté, Lucie Pastor, Yves Thiry, Françoise Siclet, and Jérôme Balesdent. 2016. 'Hydrogen Dynamics in Soil Organic Matter as Determined by 13C and 2H Labeling

https://doi.org/10.5194/egusphere-2026-1312
Preprint. Discussion started: 23 March 2026
© Author(s) 2026. CC BY 4.0 License.

Experiments'. *Biogeosciences* 13 (24): 6587–98. https://doi.org/10.5194/BG-13-6587-2016.

Paulot, Fabien, David Paynter, Vaishali Naik, Sergey Malyshev, Raymond Menzel, and Larry W. Horowitz. 2021. 'Global Modeling of Hydrogen Using GFDL-AM4.1: Sensitivity of Soil Removal and Radiative Forcing'. *International Journal of Hydrogen Energy* 46 (24): 13446–60. https://doi.org/10.1016/J.IJHYDENE.2021.01.088.

Pendall, E., L. Schwendenmann, T. Rahn, J. B. Miller, P. P. Tans, and J. W. C. White. 2010. 'Land Use and Season Affect Fluxes of CO2, CH4, CO, N2O, H2 and Isotopic Source Signatures in Panama: Evidence from Nocturnal Boundary Layer Profiles'. *Global Change Biology* 16 (10): 2721–36. https://doi.org/10.1111/j.1365-2486.2010.02199.x.

Pétron, Gabrielle, Andrew M. Crotwell, John Mund, Molly Crotwell, Thomas Mefford, Kirk Thoning, Bradley Hall, et al. 2024. 'Atmospheric H_2 Observations from the NOAA Cooperative Global Air Sampling Network'. *Atmospheric Measurement Techniques* 17 (16): 4803–23. https://doi.org/10.5194/amt-17-4803-2024.

Piché-Choquette, Sarah, and Philippe Constant. 2019. 'Molecular Hydrogen, a Neglected Key Driver of Soil Biogeochemical Processes'. *Applied and Environmental Microbiology* 85 (6): e02418-18. https://doi.org/10.1128/AEM.02418-18.

Piché-Choquette, Sarah, Julien Tremblay, Susannah G. Tringe, and Philippe Constant. 2016. 'H2-Saturation of High Affinity H2-Oxidizing Bacteria Alters the Ecological Niche of Soil Microorganisms Unevenly among Taxonomic Groups'. *PeerJ* 4 (March):e1782. https://doi.org/10.7717/peerj.1782.

Poulter, B. 2021. 'LPJ Dynamic Global Vegetation Model: NPP Output, TRENDYv10 (LPJ_S0_npp.Nc)'. NASA / TRENDYv10 Project. https://doi.org/Contact: benjamin.poulter@nasa.gov.

Reji, Linta, Matteo B. Bertagni, Fabien Paulot, Qianhui Qin, and Xinning Zhang. 2025. 'Global Implications of a Low Soil Moisture Threshold for Microbial Hydrogen Uptake'. *Nature Communications* 17 (1): 515. https://doi.org/10.1038/s41467-025-67208-3.

Sand, Maria, Ragnhild Bieltvedt Skeie, Marit Sandstad, Srinath Krishnan, Gunnar Myhre, Hannah Bryant, Richard Derwent, et al. 2023. 'A Multi-Model Assessment of the Global Warming Potential of Hydrogen'. *Communications Earth & Environment* 4 (1): 1–12. https://doi.org/10.1038/s43247-023-00857-8.

Sanderson, M. G., W. J. Collins, R. G. Derwent, and C. E. Johnson. 2003. 'Simulation of Global Hydrogen Levels Using a Lagrangian Three-Dimensional Model'. *Journal of Atmospheric Chemistry* 46:15–28.

Schjønning, Per, Jan JH van den Akker, Thomas Keller, Mogens H Greve, Mathieu Lamandé, Asko Simojoki, Matthias Stettler, Johan Arvidsson, and Henrik Breuning-Madsen. 2015. 'Driver-Pressure-State-Impact-Response (DPSIR) Analysis and Risk Assessment for Soil Compaction—a European Perspective'. *Advances in Agronomy* 133:183–237.

Smith Downey, Nicole V. 2007. 'Soil Uptake of Molecular Hydrogen and Remote Sensing of Soil Freeze and Thaw'. Phd, California Institute of Technology. https://doi.org/10.7907/BXV8-HH61.

Smith, Jo, Dali Nayak, Ashim Datta, Wasudeo Nivrutti Narkhede, Fabrizio Albanito, Bedru Balana, Sanjoy K. Bandyopadhyay, Helaina Black, Shiferaw Boke, and Alison Brand. 2020. 'A Systems Model Describing the Impact of Organic Resource Use on Farming Households in Low to Middle Income Countries'. *Agricultural Systems* 184:102895.

Smith-Downey, Nicole V., James T. Randerson, and John M. Eiler. 2006. 'Temperature and Moisture Dependence of Soil H_2 Uptake Measured in the Laboratory'. *Geophysical Research Letters* 33 (14): L14813. https://doi.org/10.1029/2006GL026749.

Smith-Downey, Nicole V., James T. Randerson, and John M. Eiler. 2008. 'Molecular Hydrogen Uptake by Soils in Forest, Desert, and Marsh Ecosystems in California'. *Journal of Geophysical Research* 113 (G3): G03037. https://doi.org/10.1029/2008JG000701.

https://doi.org/10.5194/egusphere-2026-1312
Preprint. Discussion started: 23 March 2026
© Author(s) 2026. CC BY 4.0 License.

1043 Strudley, Mark W, Timothy R Green, and James C Ascough II. 2008. 'Tillage Effects on Soil
1044 Hydraulic Properties in Space and Time: State of the Science'. *Soil and Tillage Research*
1045 99 (1): 4–48.
1046 Totsche, Kai Uwe, Wulf Amelung, Martin H Gerzabek, Georg Guggenberger, Erwin Klumpp,
1047 Claudia Knief, Eva Lehndorff, Robert Mikutta, Stephan Peth, and Alexander Prechtel.
1048 2018. 'Microaggregates in Soils'. *Journal of Plant Nutrition and Soil Science* 181 (1): 104–
1049 36.
1050 Yonemura, Seiichiro, Masayuki Yokozawa, S. Kazuhiko, and H. Tsuruta. 2000. 'Model Analysis of
1051 the Influence of Gas Diffusivity in Soil on CO and H 2 Uptake'. *Tellus B* 52 (3).
1052 https://doi.org/10.1034/j.1600-0889.2000.d01-2.x.
1053 Young, Iain M, and John W Crawford. 2004. 'Interactions and Self-Organization in the Soil-Microbe
1054 Complex'. *Science* 304 (5677): 1634–37.
1055